

# Greedy Search Algorithms for Unsupervised Variable Selection: A Comparative Study

Federico Zocco<sup>a</sup>, Marco Maggipinto<sup>b</sup>, Gian Antonio Susto<sup>b</sup>, Seán McLoone<sup>a</sup>

<sup>a</sup>*Centre for Intelligent Autonomous Manufacturing Systems (i-AMS), Queen's University Belfast, Northern Ireland, UK; email: {fzocco01,s.mcloone}@qub.ac.uk*

<sup>b</sup>*Department of Information Engineering, University of Padua, Italy; email: {marco.maggipinto,gianantonio.susto}@dei.unipd.it*

---

## Abstract

Dimensionality reduction is an important step in the development of scalable and interpretable data-driven models, especially when there are a large number of candidate variables. This paper focuses on unsupervised variable selection based dimensionality reduction, and in particular on *unsupervised greedy* selection methods, which have been proposed by various researchers as computationally tractable approximations to optimal subset selection. These methods are largely distinguished from each other by the selection criterion adopted, which include squared correlation, variance explained, mutual information and frame potential. Motivated by the absence in the literature of a systematic comparison of these different methods, we present a critical evaluation of seven unsupervised greedy variable selection algorithms considering both simulated and real world case studies. We also review the theoretical results that provide performance guarantees and enable efficient implementations for certain classes of greedy selection function, related to the concept of submodularity. Furthermore, we introduce and evaluate for the first time, a lazy implementation of the variance explained based forward selection component analysis (FSCA) algorithm. Our experimental results show that: (1) variance explained and mutual information based selection methods yield smaller approximation errors than frame potential; (2) the lazy FSCA implementation has similar performance to FSCA, while being an order of magnitude faster to compute, making it the algorithm of choice for unsupervised variable selection.

*Keywords:* Greedy algorithm, variable selection, feature selection, submodular function, submodularity.

---

## 1. Introduction

In recent years, the big data revolution has paved the way for the diffusion of data-driven technologies for a whole range of heterogeneous applications. Data-driven solutions have been proposed in biology [1, 2], manufacturing [3, 4], and finance [5, 6], for example, and their popularity can be attributed to the combined effect of three factors: (1) the availability of large amounts of data enabled by the proliferation of sensors for system monitoring; (2) the major advances in data analysis and Machine Learning (ML) algorithms that have transformed our ability to model and extract useful information from data; (3) the accessibility of affordable computing resource from stand-alone high performance PCs and GPUs to cloud based platforms that have made large scale data processing and complex algorithm execution computationally feasible.

When dealing with high dimensional datasets, unsupervised dimensionality reduction is often performed as a pre-processing step to achieve efficient storage of the data and robustness of ML algorithms. The underlying assumption is that such datasets have high levels of correlation among variables and hence redundancy that can be exploited. Principal Component Analysis (PCA) is the most popular linear technique for unsupervised dimensionality reduction [7], consisting of the transformation of variables into a set of orthogonal components that correspond to the directions of maximum variance in the data. These components are ordered according to their contribution to the total variance in the dataset allowing the least informative ones to be identified and removed. While PCA is a relatively simple linear projection method, its performance is often competitive even when compared with nonlinear approaches [8].

In some applications it is desirable to achieve unsupervised dimensionality reduction through the selection of a subset of initial variables that best represent the information contained in the full dataset, for example in sensor selection

problems [9, 10]. Working with a subset of the original variables also facilitates more transparent and interpretable models than those based on principal components [11]. The unsupervised variable selection problem may be formulated as follows. Given a dataset  $\mathbf{X} \in \mathbb{R}^{m \times v}$  containing  $m$  measurements of  $v$  variables, and the index set for the variables (i.e. columns of  $\mathbf{X}$ )  $I_X = \{1, 2, \dots, v-1, v\}$  and defining  $I_S$  and  $I_U$  as the indices of the selected and unselected variables ( $I_S \cup I_U = I_X$ ), respectively, we wish to solve

$$I_S^* = \underset{I_S \subset I_X}{\operatorname{argmax}} g(I_S) \quad \text{s.t.} \quad |I_S| = k \quad (1)$$

where  $I_S^*$  denotes the optimum subset,  $k$  is a cardinality constraint on  $I_S$  and  $g(\cdot): 2^v \mapsto \mathbb{R}$  is a performance metric (set function) which measures the suitability of the selected variables. An alternative formulation of the variable selection problem places a constraint  $\tau$  on the target value for the performance metric, that is:

$$I_S^* = \underset{I_S \subset I_X}{\operatorname{argmin}} |I_S| \quad \text{s.t.} \quad g(I_S) > \tau \quad (2)$$

Finding the optimal subset of variables from a set of candidate variables is an NP-hard combinatorial problem and therefore intractable in practice even for relatively low dimension problems. Consequently, developing computationally efficient techniques that approximate the optimum solution have been the focus of research for many years. Existing techniques can be split into four categories: PCA-based methods, convex relaxations of the cardinality constraint, non-convex relaxations of the cardinality constraint and greedy search methods. In PCA-based variable selection methods the basic PCA formulation is modified to encourage sparsity in the principal components, thereby allowing subsets of the variables that contribute most towards the directions of maximum variance in the data to be identified, e.g. SCoTLASS [12], DSPCA [13], sparse PCA [14], and SOCA [15]. Examples of convex optimization relaxations of the cardinality constraint include [16, 17] who formulate sensor selection as optimising a selection vector  $\mathbf{w}$  subject to a Boolean constraint  $\mathbf{w} \in \{0, 1\}^v$  which they then relax to be a convex box constraint  $\mathbf{w} \in [0, 1]^v$ , [18] who replace the non-convex  $L_0$ - (quasi) norm with the convex  $L_1$ -norm in their optimisation objective, and [19]

who obtain a convex principal feature selection algorithm by introducing a sparsity inducing  $L_1$ -norm penalty term in their problem formulation. *Non-convex optimization relaxations of the cardinality constraint* are typically achieved by introducing a sparsity inducing regularization term in the performance metric (cost function) being optimised. Notable examples of this approach include the *nonnegative garrote* employed for input variable selection in neural networks by [20], the integration of the LASSO variable selection approach with MLP training by [21], and the imposition of a row-sparse regularisation term on the input weights of an autoencoder neural network for unsupervised variable selection by [22].

Forward greedy search methods, which are the focus of this study, estimate the optimum subset of variables by recursively adding them one at a time, such that the variable added at each iteration is the one that gives the optimal improvement in the chosen performance metric  $g(\cdot)$ . Examples of this approach can be found in [23, 24, 25, 26]. The general structure of a forward greedy selection algorithm for Eq. (1) is as defined in Algorithm 1. The corresponding greedy algorithm for solving Eq. (2) can be obtained by replacing the while loop condition in line 2 with  $g(I_S) < \tau$ .

---

**Algorithm 1** Forward greedy variable selection

---

**Input:**  $\mathbf{X}, k$

- 1:  $I_U = \{1, 2, \dots, v - 1, v\}; I_S = \emptyset$
  - 2: **while**  $|I_S| < k$  **do**
  - 3:      $i^* = \operatorname{argmax}_{i \in I_U} \{g(I_S \cup \{i\})\}$
  - 4:      $I_S = I_S \cup \{i^*\}; I_U = I_U \setminus \{i^*\}$
  - 5: **end while**
  - 6: **return**  $I_S$
- 

While not guaranteed to be optimal, greedy search methods have grown in popularity due to their intuitive nature, low computational complexity, potential for parallel implementation relative to alternative approaches, and the reassurance of strong theoretical guarantees for certain classes of performance

metric. In particular, if  $g(\cdot)$  is a *monotone increasing, submodular*<sup>1</sup> metric and  $g(\emptyset) = 0$ , then the greedy search solution  $g(I_S)$  is guaranteed to be within 63% of the optimal solution and a highly efficient implementation of the greedy search algorithm, referred to as the *lazy greedy* implementation [27], is possible.

Several greedy search based unsupervised variable selection algorithms have been proposed in the literature using a number of different performance metrics. *Variance explained* (VE) was employed in the forward selection component analysis (FSCA) algorithm introduced in [24, 28], while the squared multiple correlation was employed by [29] in their forward orthogonal selection maximising overall dependency (FOS-MOD) algorithm. VE also underpins the orthogonal principal feature selection (PFS) of [23] where variables are selected based on their correlation with the first principal component of the subspace orthogonal to that spanned by the currently selected variables, while the unsupervised forward selection (UFS) algorithm by Whitley et al. [30] selects the variables having the lowest squared multiple correlation with the subspace spanned by the currently selected variables. These metrics are natural choices for unsupervised variable selection given their close relationship with linear regression and PCA, however, they are not submodular functions.

Motivated by the desire to have the aforementioned performance guarantee and efficient algorithm implementation that follow from submodularity, [9] used *mutual information* (MI), [31] used *frame potential* (FP) and [16, 25] used *log-det* as submodular metrics to design near-optimal greedy sensor selection algorithms. The application areas were monitoring of spatial phenomena that can be modelled as Gaussian processes [9], linear inverse problems [31] and non-linear measurement models with additive Gaussian noise [16, 25], respectively.

To date the literature lacks a systematic comparison of the main unsupervised greedy selection algorithms with regard to the trade-off in performance when using VE, MI or FP to guide variable selection. There is also a lack of awareness of the benefit of using the lazy greedy algorithm even when submodu-

---

<sup>1</sup>Formally defined in Section 2.

larity does not apply. While VE does not satisfy the conditions for submodularity, and therefore does not enjoy convenient to compute theoretical bounds on its performance, practical experience shows that greedy search algorithms based on VE perform very well. This may mean that for many problems VE is close to being submodular, and indeed, as observed by [32], it is provably so in certain cases, and hence the lazy greedy algorithm can be expected to yield similar results to the standard greedy version. A comparison between the performance of lazy greedy and greedy implementations can be used as an indication of how close to submodular a metric is for a given problem.

Motivated by these observations, this paper makes the following contributions:

- A systematic comparison is presented of the main unsupervised greedy variable selection algorithms proposed in the literature, namely, FSCA, FOS-MOD, PFS, UFS, ITFS (based on MI), and FSFP [33] (based on FP). Specifically, the algorithms are formalised within a common framework and their performance evaluated with respect to Big-O computational complexity and the aforementioned performance metrics (VE, MI and FP) on a diverse set of simulated and real world benchmark datasets.
- The pertinent theoretical results on performance bounds that apply to greedy variable selection algorithms are presented and compared.
- A lazy greedy implementation of FSCA (the lazy FSCA algorithm) is introduced and its performance compared to conventional FSCA.
- An enhanced implementation of FSFP [33] incorporating an initial FSCA step is proposed. The algorithm, referred to as FSFP-FSCA, addresses a non-uniqueness issue that arises when selecting the first variable using FSFP.

In addition, to facilitate benchmarking against other unsupervised variable selection algorithms in the future, the code for the algorithms and experimental studies presented in the paper have been made available on GitHub<sup>4</sup>.

The remainder of the paper is organised as follows: Section 2 provides a summary and comparative evaluation of the main theoretical results on performance guarantees that apply to the unsupervised variable selection problem at hand, and introduces the lazy greedy algorithm that can be exploited when selection metrics are submodular. Section 3 then briefly introduces the unsupervised variable selection algorithms and performance metrics under investigation and provides an analysis of their computational complexity. The performance comparison on simulated and real datasets is presented in Section 4 and conclusions are provided in Section 5. The following notation is adopted: matrices and vectors are indicated with bold capital and lower case letters, respectively, while sets and scalars are denoted by capital and lower case letters, respectively.

## 2. Underpinning Theory

### 2.1. Theoretical Guarantees on Performance

Let  $v$ ,  $k$ ,  $I_S$  and  $I_S^*$  denote the total number of candidate variables, the number of selected variables, the index set of the variables selected via greedy search and the corresponding optimal index set, respectively. If the greedy unsupervised variable selection metric  $g(\cdot)$  is a monotone increasing, submodular set function and  $g(\emptyset) = 0$ , then, according to the seminal result by Nemhauser et al. [34], the greedy search solution  $g(I_S)$  is guaranteed to be within 63% of the optimal solution, or more specifically:

$$\mathcal{B}_N : \frac{g(I_S)}{g(I_S^*)} \geq 1 - \left(\frac{k-1}{k}\right)^k \geq 1 - 1/e \geq 0.63 \quad (3)$$

Set function  $g(\cdot)$  is defined as being *monotone increasing* if  $\forall A \subseteq B \subseteq X$ , it holds that  $g(A) \leq g(B)$ . It is defined as *submodular* [32] if  $\forall A \subseteq B \subseteq X, \forall x \in X \setminus B$  it satisfies the property

$$g(A \cup \{x\}) - g(A) \geq g(B \cup \{x\}) - g(B) \quad (4)$$

If the condition in Eq. (4) holds with equality then  $g(\cdot)$  is a *modular* function and the greedy solution is guaranteed to be the optimal solution, i.e.  $g(I_S) = g(I_S^*)$ .

In order to improve on  $\mathcal{B}_N$  and obtain results for more general forms of set function the concepts of *curvature* [35, 36, 37] and *submodularity ratio* [38, 39] have been introduced as measures of how far a submodular function is from being modular and how far a non-submodular function is from being submodular, respectively. Bian et al. [40] recently provided a unified treatment of these concepts and showed that if  $g(\cdot)$  is a non-negative non-decreasing set function with curvature  $\alpha \in [0, 1]$  defined as

$$\alpha = \max_{\substack{i,A,B \\ i \in X, AC \subseteq B \subseteq X/i}} \left[ 1 - \frac{g(B \cup \{i\}) - g(B)}{g(A \cup \{i\}) - g(A)} \right] \quad (5)$$

and submodularity ratio  $\gamma \in [0, 1]$  defined as

$$\gamma = \min_{\substack{A,B \\ AC \subseteq X, B \subseteq X/A}} \left[ \frac{\sum_{i \in B} (g(A \cup \{i\}) - g(A))}{g(A \cup B) - g(A)} \right] \quad (6)$$

then the following lower bound applies to the greedy solution

$$\mathcal{B}_{\alpha\gamma} : \frac{g(I_S)}{g(I_S^*)} \geq \frac{1}{\alpha} \left[ 1 - \left( \frac{k - \alpha\gamma}{k} \right)^k \right] \geq \frac{1}{\alpha} (1 - e^{-\alpha\gamma}) \quad (7)$$

When  $\gamma=1$ ,  $g(\cdot)$  is submodular. If  $\gamma=1$  and  $\alpha=1$ ,  $\mathcal{B}_{\alpha\gamma}$  yields Nemhauser et al.'s bound (Eq. 3) and if  $\alpha=0$ ,  $g(\cdot)$  is *supermodular* and  $\mathcal{B}_{\alpha\gamma}$  reduces to

$$\lim_{\alpha \rightarrow 0} \frac{1}{\alpha} (1 - e^{-\alpha\gamma}) = \gamma \quad (8)$$

Finally, when  $\alpha=0$  and  $\gamma=1$ ,  $g(\cdot)$  is modular and  $g(I_S) = g(I_S^*)$ .

Other definitions of curvature have also been introduced for non-submodular functions and used as a measure of how close a function is to being submodular [37, 41, 42]. Sviridenko et al.[37] define the curvature  $c \in [0, 1]$  for arbitrary monotone functions as

$$c = \max_{\substack{i,A,B \\ i \in X, A, B \subseteq X/i}} \left[ 1 - \frac{g(B \cup \{i\}) - g(B)}{g(A \cup \{i\}) - g(A)} \right] \quad (9)$$

and prove that greedy search maximisation of a monotone increasing function with curvature  $c$  is bounded by

$$\mathcal{B}_c : \frac{g(I_S)}{g(I_S^*)} \geq 1 - c \quad (10)$$



Comparing Eq. (5) and Eq. (9) it is apparent that maximisation is performed over a narrower range in Bian et al.'s definition of curvature than in Sviridenko et al.'s definition, hence it follows that  $c \geq \alpha$ . For submodular functions ( $\gamma = 1$ )  $\mathcal{B}_{\alpha\gamma}$  is a strictly tighter bound than  $\mathcal{B}_c$ , i.e.  $1 - c \leq 1 - \alpha < \frac{1}{\alpha}(1 - \exp(-\alpha))$  for  $\alpha > 0$ , while for non-submodular functions ( $\gamma < 1$ ) it is a tighter bound (i.e.  $\mathcal{B}_{\alpha\gamma} > \mathcal{B}_c$ ) when  $\alpha > \frac{2-2\gamma}{2\kappa-\gamma^2}$  (approximately <sup>2</sup>), where  $\kappa = \frac{c}{\alpha} \geq 1$ .

Wang et al.[41] define *elemental curvature*  $e_c \in [0, \infty)$  as

$$e_c = \max_{\substack{i,j,A \\ i,j \in X, A \subseteq X/\{i,j\}}} \left[ \frac{g(A \cup \{i, j\}) - g(A \cup \{i\})}{g(A \cup \{j\}) - g(A)} \right] \quad (11)$$

which takes values between 0 and 1 for submodular functions, and values greater than 1 for non-submodular functions. Using this definition of curvature they derive a performance bound for greedy selection which can be expressed as

$$\mathcal{B}_{e_c} : \frac{g(I_S)}{g(I_S^*)} \geq 1 - \left( \frac{e_c^k - e_c}{e_c^k - 1} \right)^k \geq 0 \quad (12)$$

for  $e_c \neq 1$  and as Nemhauser et al.'s bound ( $\mathcal{B}_N$ ) when  $e_c = 1$ . This provides a tighter bound than  $\mathcal{B}_N$  for submodular functions, but is also valid for non-submodular functions. In [26], Hashemi et al. employ an *element-wise curvature* expression, also referred to as the *weak submodularity constant* [42],  $s_c \in [0, \infty)$ , defined as

$$s_c = \max_{\substack{i,A,B \\ i \in X, A \subseteq B \subseteq X/\{i\}}} \left[ \frac{g(B \cup \{i\}) - g(B)}{g(A \cup \{i\}) - g(A)} \right] \quad (13)$$

with an associated greedy search performance guarantee of

$$\mathcal{B}_{s_c} : \frac{g(I_S)}{g(I_S^*)} \geq 1 - \left( \frac{\max(s_c, 1) - k^{-1}}{\max(s_c, 1)} \right)^k \geq 1 - e^{-\frac{1}{\max(s_c, 1)}} \quad (14)$$

A function is submodular if  $s_c \leq 1$  and non-submodular otherwise. Figure 1 shows the evolution of  $\mathcal{B}_{e_c}$  and  $\mathcal{B}_{s_c}$  with  $k$  for different values of  $e_c$  and  $s_c$  revealing that  $\mathcal{B}_{e_c}$  provides a much tighter bound for submodular functions ( $e_c, s_c < 1$ ) but is problematic for  $e_c > 1$  as it falls to zero rapidly with increasing

---

<sup>2</sup>The limiting value  $\frac{2-2\gamma}{2\kappa-\gamma^2}$ , which is obtained by employing a quadratic approximation for  $\exp(-\alpha\gamma)$ , is an upper bound on the true limit value.

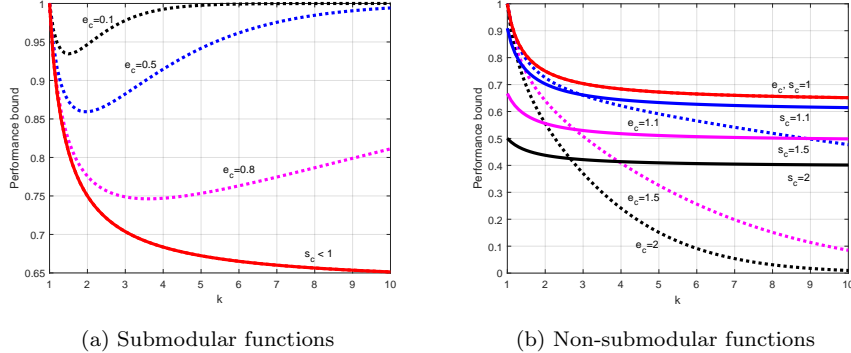


Figure 1: Comparisons of the greedy search performance bounds obtained with Wang et al’s bound ( $\mathcal{B}_{e_c}$ , dashed) and Hashemi et al’s bound ( $\mathcal{B}_{s_c}$ , solid) for different values of the elemental curvature constant  $e_c$  and weak submodularity constant  $s_c$ , respectively.

$k$ . When  $e_c = s_c$  bound  $\mathcal{B}_{s_c}$  is superior for  $k > 2$ . However, since the range over which maximisation is performed in Eq. 11 is a subset of the range  $c$  considered in Eq. 13 it follows that  $s_c \geq e_c$  and hence the value of  $k$  at which  $\mathcal{B}_{s_c}$  becomes superior may be greater, and is problem dependent.

It should be noted that even when  $g(\cdot)$  is not a modular or submodular set function in general it may have these properties for restricted forms of  $X$ . For example, while variance explained (squared multiple correlation) is not a submodular function, Das et al. [32] show that if  $X$  does not contain any suppressor variables, then  $g(\cdot)$  will be submodular and Nemhauser et al.’s performance bound  $\mathcal{B}_N$  applies. Similarly, if  $X$  is a set of uncorrelated variables, i.e  $\mathbf{X}$  is an orthogonal matrix, then  $g(\cdot)$  will be modular and the greedy search algorithm yields the optimal solution.

## 2.2. Comparison of bounds on simulated datasets

To get a sense of the relative strength of the different theoretical performance bounds for unsupervised greedy selection, the values of their characterising parameters  $\alpha$ ,  $\gamma$ ,  $c$ ,  $e_c$  and  $s_c$  are presented in Table 1 for the submodular FP and non-submodular VE metrics for four different simulated datasets, and the corresponding bounds are presented in Fig. 2. The simulated datasets were

Table 1: Parameters  $\alpha$ ,  $\gamma$ ,  $c$ ,  $e_c$  and  $s_c$  for the Frame Potential (FP) and Variance Explained (VE) variable selection metrics for 4 case study datasets.

Case study	Frame Potential					Variance Explained				
	$\alpha$	$c$	$\gamma$	$e_c$	$s_c$	$\alpha$	$c$	$\gamma$	$e_c$	$s_c$
<b>1</b>	0.914	0.914	1.000	0.999	0.999	1.000	1.000	0.591	2.760	2.760
<b>2</b>	0.964	0.964	1.000	0.997	0.997	0.999	0.999	0.754	1.995	1.995
<b>3</b>	0.802	0.802	1.000	0.999	0.999	0.912	0.912	0.852	1.642	1.673
<b>4</b>	0.115	0.115	1.000	1.000	1.000	0.115	0.115	1.000	1.001	1.001

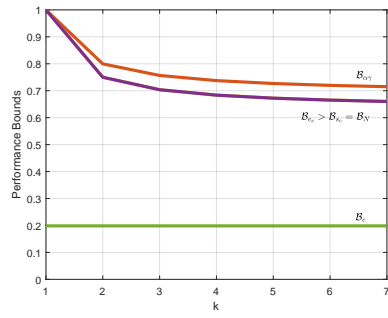
generated as

$$\mathbf{X} = (1 - \sigma)\mathbf{\Theta}\mathbf{Z} + \sigma\mathbf{\Phi}$$

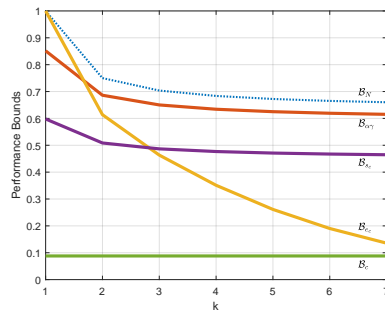
where  $\mathbf{Z} \in \mathbb{R}^{r \times v}$ ,  $\mathbf{\Theta} \in \mathbb{R}^{m \times r}$  and  $\mathbf{\Phi} \in \mathbb{R}^{m \times v}$  are randomly generated matrices, that is,  $z_{ij}, \theta_{ij}$  and  $\phi_{ij} \sim N(0, 1)$ . The case studies correspond to different  $\sigma$  and  $r$  parameter combinations as follows:

- Case study 1 ( $r = 3, \sigma = 0$ ): a correlated rank deficient matrix
- Case study 2 ( $r = 3, \sigma = 0.1$ ): a weighted combination of a correlated low rank matrix and an uncorrelated full rank matrix.
- Case study 3 ( $r = 7, \sigma = 0$ ): a correlated full rank matrix
- Case study 4 ( $r = 7, \sigma = 1, v = 7$ ): an uncorrelated full rank matrix.

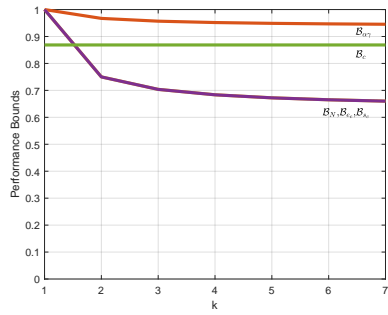
The results in Table 1, which are for  $v = 7$  and  $m = 100$ , are representative of the patterns observed for experiments conducted across a range of  $v$  and  $m$  values ( $5 \leq v \leq 12, m \in \{50, 100, 500\}$ ). The main patterns to note are that  $\alpha = c$  in all case studies, but occasionally  $s_c > e_c$ . For the FP metric, submodularity is confirmed with  $\gamma = 1$  and  $e_c \leq 1$  and  $s_c \leq 1$  for all case studies. In contrast, for VE  $\gamma < 1$  for case studies 1, 2 and 3 which correspond to the correlated datasets and is equal to 1 for case study 4, the randomly generated dataset. This case study also has a much lower  $\alpha$  value than the other case studies due to the tendency of randomly generated column vectors to be uncorrelated with the result that the performance metrics tend towards



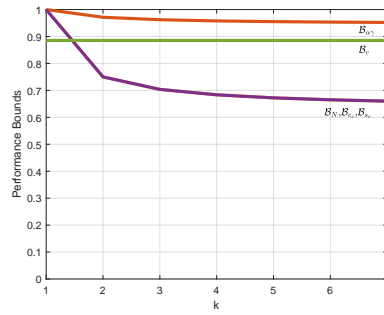
(a) FP: Case study 3



(b) VE: Case study 3



(c) FP: Case study 4



(d) VE: Case study 4

Figure 2: Comparisons of the greedy search performance bounds for case studies 3 and 4 for the Frame Potential (FP) and Variance Explained (VE) metrics.

modularity. As  $m$  is increased the sample correlation tends towards the expected value of 0, as does  $\alpha$ . For example, when  $m = 500$ ,  $\alpha < 0.05$  for both FP and VE.

The greedy search performance bounds  $\mathcal{B}_N$ ,  $\mathcal{B}_{\alpha\gamma}$ ,  $\mathcal{B}_c$ ,  $\mathcal{B}_{e_c}$  and  $\mathcal{B}_{s_c}$  are plotted in Fig. 2 for case studies 3 and 4. The plots for case study 3 (Fig. 2(a) and Fig. 2(b)) are representative of the patterns observed for all three correlated datasets, hence plots for case study 1 and 2 are omitted for conciseness. For the submodular performance metric (FP) and the case study where the structure of the dataset induces submodularity (case study 4) Wang et al.’s [41], Hessema et al.’s [42] and Nemhauser’s [34] bounds are indistinguishable. However, while not visible in the plots,  $\mathcal{B}_{e_c}$  is marginally superior to the other bounds when  $e_c < 1$ , i.e.  $\mathcal{B}_{e_c} \geq \mathcal{B}_{s_c} = \mathcal{B}_N$ . In all these cases  $\mathcal{B}_{\alpha\gamma}$ , the bound proposed by Bain et al. [40], is the best performing (tightest) bound. It is substantially superior to the other bounds in case study 4 as it takes account of the close to modular nature of this problem (i.e.  $\alpha \ll 1$ ). Sviridenko et al.’s [37] bound is also able to reflect the close to modular nature of case study 4 yielding a tighter bound than the  $1 - e^{-1}$  bound of Nemhauser’s [34]. However, it is the worst performing bound for the other cases studies. The greatest differences between the bounds occurs with VE in case study 3 (Fig. 2(b)). This problem is not submodular ( $\gamma < 1$ ) with the result that Nemhauser’s bound [34] does not apply. Here,  $\mathcal{B}_{\alpha\gamma}$  again provides the tightest bound, followed by  $\mathcal{B}_{e_c}$  for  $k < 3$  and  $\mathcal{B}_{s_c}$  otherwise.

In general, computing the constants  $\alpha$ ,  $\gamma$ ,  $c$ ,  $e_c$  and  $s_c$  is as computationally intractable as the original subset selection problem. For example, computing the values for a single case study in Table 1 ( $v = 7$ ) took approximately 7 seconds per metric on a standard PC. The results for  $v = 10$  took 10 minutes to compute. Determining the values for  $v = 15$  would take 14 days and for  $v = 20$  variables the estimated computation time is 69 years.<sup>3</sup> Hence de-

---

<sup>3</sup>These estimates were obtained by fitting the computation times ( $T$ ) for the datasets with  $v = 5, 6, \dots, 12$  to an exponential model  $T(v) = a \cdot b^{v-10}$  and then using this model to extrapolate. The total computation time model parameters were  $a = 640$ ,  $b = 4.5$ . These were

terminating the associated lower bounds  $\mathcal{B}_{\alpha\gamma}$ ,  $\mathcal{B}_c$ ,  $\mathcal{B}_{e_c}$  and  $\mathcal{B}_{s_c}$  is not feasible even for modestly sized problems. However, for specific problem formulations bounds can be computed for the curvature and submodularity ratio parameters that are computationally tractable, allowing weaker versions of the performance guarantees to be computed. For example, Bian et al. [40] develop bounds for  $\alpha$  and  $\gamma$  for A-optimal design of experiments, determinantal function and linear programme with constraints based problems, Das and Kempe [38] show that for VE based regression problems  $\gamma$  can be lower bounded by the smallest eigenvalue of the normalised data covariance matrix, and Hashemi et al. [26] show that  $s_c$  can be upperbounded by an expression in terms of the maximum and minimum values of the Kalman filter error covariance matrix in a state estimation sensor selection problem.

### 2.3. Lazy Greedy Implementation

Submodularity is essentially a diminishing returns property. Defining the *marginal gain* (improvement in performance) of adding  $x$  to  $I_S$  at the  $k$ -th iteration of the greedy search algorithm as

$$\Delta g_k(x) = g(I_S \cup \{x\}) - g(I_S), \quad (15)$$

Eq. (4) implies that  $\Delta g_j(x) \leq \Delta g_k(x)$  for  $\forall j > k$ , that is, the marginal gain achievable with a given variable decreases (or at best remains the same) the later in the sequence it is added. Consequently, the marginal gain given by an element, i.e. variable,  $x$  at the current iteration is an upper bound on its marginal gain at subsequent iterations. This property can be exploited to arrive at a greedy search algorithm for submodular functions that has much lower computational complexity than the conventional greedy search algorithm, as first proposed by Minoux [27]. The algorithm, usually referred to as the lazy greedy search algorithm, operates by maintaining a descending-ordered list of

---

largely determined by the computation of  $c$  which had an exponential growth rate ( $b$ ) of 4.7. The exponential growth rates for  $\alpha$ ,  $s_c$ ,  $\gamma$  and  $e_c$  were 3.5, 3.5, 3.3 and 2.6, respectively.

the upper bounds on the marginal gain of each candidate variable (which is initialized at the first iteration), and then, at each iteration, computing the marginal gains sequentially from the top of the list until a candidate variable is found whose *marginal gain* is greater than the next largest *upper bound* in the list. In this way, the number of set function evaluations required to identify the best candidate variable at each iteration can be substantially reduced.

The pseudocode for a lazy greedy variable selection algorithm is given in Algorithm 2. Here  $G_U^o$  is a decreasing-ordered list of the marginal gain bounds for the set of currently unselected candidate variables,  $I_U^o$  is the corresponding index set, and  $EB_{\text{flag}}^o$  is a Boolean set used to track which entries in the ordered list are exact marginal gains ( $= 1$ ) and which are upper bounds ( $= 0$ ). The function  $\text{reorder}(\cdot)$  is used to denote the insertion of the updated marginal gain value in the appropriate location in the ordered list and the corresponding reordering of the entries in  $I_U^o$  and  $EB_{\text{flag}}^o$ . This step can be efficiently implemented taking advantage of the existing ordering of the lists.

### 3. Candidate Algorithms

This section provides a description of the six baseline algorithms of our comparative study along with a computational complexity analysis. Without loss of generality, the data matrix  $\mathbf{X}$  is assumed to have mean-centered columns.

#### 3.1. Forward Selection Component Analysis (FSCA)

FSCA [24], first proposed in [43] in the context of optical emission spectroscopy channel selection, has been found to be an effective tool for data-driven metrology plan optimization in the semiconductor manufacturing industry [10, 28, 44]. The algorithm, which can be regarded as the unsupervised counterpart of forward selection regression [45], selects, in a greedy fashion, the variables that provide the greatest contribution to the variance in the dataset  $\mathbf{X}$ . As depicted in Algorithm 3, FSCA operates recursively selecting, at each iteration, the variable that maximizes the variance explained with respect to the

---

**Algorithm 2** Lazy greedy variable selection

---

**Input:**  $\mathbf{X}, k$ 

- 1:  $I_U = \{1, 2, \dots, v-1, v\}; I_S = \emptyset$
  - 2:  $G_U = \{g(i) - g(\emptyset), i \in I_U\}$
  - 3:  $[I_U^o, G_U^o] = \text{sort}(G_U)$
  - 4:  $I_S = I_U^o(1); I_U(1) = \emptyset; G_U^o(1) = \emptyset$
  - 5: **while**  $|I_S| < k$  **do**
  - 6:      $EB_{\text{flag}}^o = \text{zeros}(\text{size}(I_U^o))$
  - 7:     **while**  $EB_{\text{flag}}^o(1) \neq 1$  **do**
  - 8:          $G_U^o(1) = g(I_S \cup I_U^o(1)) - g(I_S)$
  - 9:          $EB_{\text{flag}}^o(1) = 1$
  - 10:          $[I_U^o, G_U^o, EB_{\text{flag}}^o] = \text{reorder}(G_U^o)$
  - 11:     **end while**
  - 12:      $I_S = I_S \cup I_U^o(1); I_U(1) = \emptyset; G_U^o(1) = \emptyset$
  - 13: **end while**
  - 14: **return**  $I_S$
- 

residual matrix  $\mathbf{R}$  obtained by removing from  $\mathbf{X}$  the contribution of the variables selected during the previous iterations (Step 6). The variance explained (VE) performance metric is defined as

$$V_{\mathbf{R}}(\hat{\mathbf{R}}(\mathbf{r}_i)) = \left(1 - \frac{\|\mathbf{R} - \hat{\mathbf{R}}(\mathbf{r}_i)\|_F^2}{\|\mathbf{R}\|_F^2}\right) \cdot 100 \quad (16)$$

where  $\hat{\mathbf{R}}(\mathbf{r}_i)$  is the matrix  $\mathbf{R}$  reconstructed by regressing on  $\mathbf{r}_i$ , the  $i$ -th column of  $\mathbf{R}$ , i.e.

$$\hat{\mathbf{R}}(\mathbf{r}_i) = \frac{\mathbf{r}_i \mathbf{r}_i^T}{\mathbf{r}_i^T \mathbf{r}_i} \mathbf{R} \quad (17)$$

Here,  $\|\mathbf{R} - \hat{\mathbf{R}}(\mathbf{r}_i)\|_F$  is the Frobenius norm of the difference between the reconstructed and actual residual matrix. Maximising the explained variance in (16) is equivalent to maximising the Rayleigh Quotient of  $\mathbf{R}\mathbf{R}^T$  with respect to  $\mathbf{r}_i$  and this can be exploited to achieve a computationally efficient implementation of FSCA as described in [24].



In terms of the greedy search algorithm formulation in Algorithm 1, FSCA corresponds to setting  $g(I_S) = V_{\mathbf{X}}(\hat{\mathbf{X}}(\mathbf{X}_S))$ , where  $\mathbf{X}_S$  is the subset of columns of  $\mathbf{X}$  corresponding to  $I_S$  and  $\hat{\mathbf{X}}(\mathbf{X}_S)$  is the projection of  $\mathbf{X}$  on  $\mathbf{X}_S$ , that is:

$$\hat{\mathbf{X}}(\mathbf{X}_S) = \mathbf{X}_S[\mathbf{X}_S^T \mathbf{X}_S]^{-1} \mathbf{X}_S^T \mathbf{X} \quad (18)$$

A lazy greedy implementation of the FSCA algorithm can then be realised as set out in Algorithm 2. This will be referred to as L-FSCA, hereafter.

---

**Algorithm 3** FSCA

---

**Input:**  $\mathbf{X}, k$

- 1:  $I_U = \{1, 2, \dots, v-1, v\}; I_S = \emptyset$
  - 2:  $\mathbf{R}_1 = \mathbf{X}$
  - 3: **for**  $j = 1$  to  $k$  **do**
  - 4:    $i^* = \operatorname{argmax}_{i \in I_U} \{V_{\mathbf{R}_j}(\hat{\mathbf{R}}_j(\mathbf{r}_i))\}$
  - 5:    $I_S = I_S \cup \{i^*\}; I_U = I_U \setminus \{i^*\}$
  - 6:    $\mathbf{R}_{j+1} = \mathbf{R}_j - \hat{\mathbf{R}}_j(\mathbf{r}_{i^*})$
  - 7: **end for**
  - 8: **return**  $I_S$
- 

### 3.2. Forward Orthogonal Search Maximizing the Overall Dependency (FOS-MOD)

FOS-MOD, proposed by Wei et al. [29], selects the most representative variables based on their similarity with the unselected variables using the *squared correlation coefficient*. Given two vectors  $\mathbf{x}_i$  and  $\mathbf{x}_j$ , the squared correlation coefficient is defined as

$$\rho^2(\mathbf{x}_i, \mathbf{x}_j) = \frac{(\mathbf{x}_i^T \mathbf{x}_j)^2}{(\mathbf{x}_i^T \mathbf{x}_i)(\mathbf{x}_j^T \mathbf{x}_j)} \quad (19)$$

The rationale behind the algorithm is to select, at each iteration, the residual direction  $\mathbf{r}_i$  having the highest average  $\rho^2$  with the unselected variables. Hence, the variable selection function is defined as

$$\bar{C}(\mathbf{r}_i) = \frac{1}{v} \sum_{j=1}^v \rho^2(\mathbf{x}_j, \mathbf{r}_i) \quad (20)$$

Note that, since  $\mathbf{r}_i$  is orthogonal to the selected variables, the contribution of these variables to the summation is zero. The pseudocode for FOS-MOD is given in Algorithm 4.

---

**Algorithm 4** FOS-MOD

---

**Input:**  $\mathbf{X}, k$

- 1:  $I_U = \{1, 2, \dots, v-1, v\}; I_S = \emptyset$
  - 2:  $\mathbf{R}_1 = \mathbf{X}$
  - 3: **for**  $j = 1$  to  $k$  **do**
  - 4:    $i^* = \operatorname{argmax}_{i \in I_U} \{\bar{C}(\mathbf{r}_i)\}$
  - 5:    $I_S = I_S \cup \{i^*\}; I_U = I_U \setminus \{i^*\}$
  - 6:    $\mathbf{R}_{j+1} = \mathbf{R}_j - \hat{\mathbf{R}}_j(\mathbf{r}_{i^*})$
  - 7: **end for**
  - 8: **return**  $I_S$
- 

### 3.3. Information Theoretic Feature Selection (ITFS)

ITFS was originally proposed by Krause et al. [9] for a sensor placement problem where an initial sensor deployment is exploited to perform a data-driven optimal placement maximising the *mutual information* (MI) between the selected and unselected sensor locations, such that the information lost by removing a sensor at each step is minimized. Specifically, a discrete set of locations  $V$  is split into the set of selected  $S$  and unselected  $U$  locations, respectively. The goal is to place  $k$  sensors in order to have the minimal uncertainty over the unselected locations, i.e.

$$S^* = \operatorname{argmax}_{|S|=k} \{H(U) - H(U|S)\}, \quad (21)$$

where  $H(\cdot)$  is the entropy over a set. Hence,  $S^*$  is the set that maximizes the reduction of entropy (uncertainty) over the unselected locations. To achieve a mathematical expression for the MI it is assumed that the variables are distributed according to a multivariate Gaussian distribution. Under this assumption, we can employ a Gaussian process regression model [46] to estimate the

multivariate distribution of a set of unselected variables  $U$  given the selected ones in  $S$ . For a measurement vector  $\mathbf{s} \in S$  the multivariate distribution of the unmeasured variables is still multivariate Gaussian with mean  $\boldsymbol{\mu}^*$  and covariance matrix  $\boldsymbol{\Sigma}^*$ , i.e.  $\mathbf{U} \sim \mathcal{N}(\boldsymbol{\mu}^*, \boldsymbol{\Sigma}^*)$  where:

$$\boldsymbol{\mu}^* = \mathbf{K}(U, S)(\mathbf{K}(S, S) + \sigma^2 \mathbf{I})^{-1} \mathbf{s} \quad (22)$$

$$\boldsymbol{\Sigma}^* = \mathbf{K}(U, U) + \sigma^2 \mathbf{I} - \mathbf{K}(U, S)(\mathbf{K}(S, S) + \sigma^2 \mathbf{I})^{-1} \mathbf{K}(S, U) \quad (23)$$

where  $\mathbf{I} \in \mathbb{R}^{|S| \times |S|}$  and  $\mathbf{K}(\cdot, \cdot)$  is a covariance matrix that can be estimated from the available historical data. In general, given two sets of variables  $A$  and  $B$  indexed by  $I_A$  and  $I_B$ , we have

$$\mathbf{K}(A, B) = \boldsymbol{\Sigma}_{AB} = \frac{1}{m} \mathbf{X}_A^T \mathbf{X}_B \quad (24)$$

where  $\mathbf{X}_A$  and  $\mathbf{X}_B$  are the matrices formed by the columns of  $\mathbf{X}$  indexed by  $I_A$  and  $I_B$ , respectively. The hyperparameter  $\sigma$  takes into account the measurement noise. The problem of maximizing the MI belongs to the NP-complete class of problems [9], hence an approximated solution can be found using a greedy approach that sequentially selects the variable  $\mathbf{x}_i$  (i.e. the  $i$ -th column of  $\mathbf{X}$ ) that maximizes the increment in mutual information [9]:

$$\begin{aligned} \Delta_{MI}(\mathbf{x}_i) &= MI(S \cup \mathbf{x}_i; U \setminus \mathbf{x}_i) - MI(S; U) \\ &= H(\mathbf{x}_i|S) - H(\mathbf{x}_i|U \setminus \mathbf{x}_i) \end{aligned} \quad (25)$$

with the conditional distribution  $\mathbf{x}_i|U \sim \mathcal{N}(\mu_U^*, \sigma_U^*)$ , and  $\mu_U^*$  and  $\sigma_U^*$  estimated via Eq. 22 and 23. Recalling that for a Gaussian random variable  $p$ , the entropy  $H(p)$  is a function of its variance  $\sigma_p$

$$H(p) = \frac{1}{2} \ln(2\pi e \sigma_p), \quad (26)$$

Eq. 25 can be expressed as

$$\begin{aligned} \Delta_{MI}(\mathbf{x}_i) &= H(\mathbf{x}_i|S) - H(\mathbf{x}_i|U \setminus \mathbf{x}_i) \\ &= \frac{\sigma_{\mathbf{x}_i} - \boldsymbol{\Sigma}_{S\mathbf{x}_i}^T \boldsymbol{\Sigma}_{SS}^{-1} \boldsymbol{\Sigma}_{S\mathbf{x}_i}}{\sigma_{\mathbf{x}_i} - \boldsymbol{\Sigma}_{U\mathbf{x}_i}^T \boldsymbol{\Sigma}_{UU}^{-1} \boldsymbol{\Sigma}_{U\mathbf{x}_i}}. \end{aligned} \quad (27)$$

The pseudocode for ITFS is given in Algorithm 5. While MI is not in general monotonically increasing, Krause et al. [9] show that, when  $|I_S| \ll v$ , the diminishing returns property (Eq. 4) applies, hence ITFS is guaranteed to be within 63% of the optimal value in terms of the MI of  $\mathbf{X}$ .

---

**Algorithm 5** ITFS

---

**Input:**  $\mathbf{X}, k$

- 1:  $I_U = \{1, 2, \dots, v-1, v\}; I_S = \emptyset$
  - 2: **for**  $j = 1$  to  $k$  **do**
  - 3:      $i^* = \operatorname{argmax}_{\mathbf{x}_i \in U} \Delta_{MI}(\mathbf{x}_i)$
  - 4:      $I_S = I_S \cup \{i^*\}; I_U = I_U \setminus \{i^*\}$
  - 5: **end for**
  - 6: **return**  $I_S$
- 

### 3.4. Principal Feature Selection (PFS)

PFS, presented in Algorithm 6, is a PCA guided approach to variable selection introduced by Cui and Di [23]. At each iteration it selects the variable that corresponds to the residual vector  $\mathbf{r}_i$  that is most correlated with the first principal component (PC)  $\mathbf{p}_1$  of the residual matrix  $\mathbf{R}$  obtained after the contribution of the variables selected in the previous iterations has been removed (as per the matrix deflation Step at line 7 with  $\hat{\mathbf{R}}$  defined as in Eq. 17). The correlation is measured using Pearson’s correlation coefficient which, for mean-centred residual vector  $\mathbf{r}_i$  and principal component  $\mathbf{p}_1$ , is defined as

$$\rho(\mathbf{r}_i, \mathbf{p}_1) = \frac{\mathbf{r}_i^T \mathbf{p}_1}{\sqrt{(\mathbf{r}_i^T \mathbf{r}_i)(\mathbf{p}_1^T \mathbf{p}_1)}} \quad (28)$$

### 3.5. Forward Selection Frame Potential (FSFP)

The FSFP algorithm introduced in [33] was inspired by the frame potential based sensor selection method proposed by Ranieri et al [31] for linear inverse problems. The *frame potential* (FP) of a matrix  $\mathbf{X}$  is defined as

$$FP(\mathbf{X}) = \sum_{i,j=1}^v |\langle \mathbf{x}_i, \mathbf{x}_j \rangle|^2 \quad (29)$$

---

**Algorithm 6** PFS

---

**Input:**  $\mathbf{X}, k$ 

- 1:  $I_U = \{1, 2, \dots, v-1, v\}; I_S = \emptyset$
  - 2:  $\mathbf{R}_1 = \mathbf{X}$
  - 3: **for**  $j = 1$  to  $k$  **do**
  - 4:    $\mathbf{p}_1 =$  First principal component of  $\mathbf{R}_j$
  - 5:    $i^* = \operatorname{argmax}_{i \in I_U} |\rho(\mathbf{r}_i, \mathbf{p}_1)|$
  - 6:    $I_S = I_S \cup \{i^*\}; I_U = I_U \setminus \{i^*\}$
  - 7:    $\mathbf{R}_{j+1} = \mathbf{R}_j - \hat{\mathbf{R}}_j(\mathbf{r}_{i^*})$
  - 8: **end for**
  - 9: **return**  $I_S$
- 

where  $\mathbf{x}_j$  denotes the  $j$ -th column of  $\mathbf{X}$ . It is an attractive metric for variable selection as minimising FP encourages orthogonality among the selected columns of  $\mathbf{X}$ . Ranieri et al.[31] showed that the set function  $f(I_U) = FP(\mathbf{X}) - FP(\mathbf{X}_S)$ , where  $I_S = I_X \setminus I_U$ , is monotone increasing, submodular and  $f(\emptyset) = 0$ . Therefore it satisfies the conditions for Nemhauser’s bound (Eq. 3) and its greedy maximisation is guaranteed to be within 63% of the global optimum solution. However, with this formulation variable selection is achieved by backward elimination, that is, the algorithm begins with all variables selected and then unselects variables one at a time until  $k$  variables remain. Therefore, the algorithm must iterate  $v - k$  times, at which point the desired variables are given by  $I_S = I_X \setminus I_U$ . Backward elimination is computationally much more demanding than forward selection, especially when  $k \ll v$ . In our previous work [33] we propose an FP based forward selection algorithm (i.e. FSFP) where the variable selection metric is given by

$$g(I_S) = FP(\mathbf{X}) - FP(\mathbf{X}_S). \quad (30)$$

The resulting algorithm (summarised in Algorithm 7) is computationally much more efficient than backward elimination, but no longer meets the requirements for the  $\mathcal{B}_N$  bound (Eq. 3) since  $g(\cdot)$  is a monotone decreasing function and  $g(\emptyset) \neq$

0. However, submodularity does apply allowing a lazy greedy implementation.

As suggested in [31], FP-based greedy selection provides better results when matrix  $\mathbf{X}$  is normalized to have columns with unitary norm. However, this presents a challenge for FSFP as all variables have the same FP, precisely equal to one, leading to an ambiguous choice for the first variable. Different solutions can be adopted to address this ambiguity. The simplest solution is to randomly select the first variable, however this leads to an output  $I_S$  that is not unique for a given  $\mathbf{X}$ . Two alternatives are to select the optimum pair of variables instead of a single variable at the first step, or to evaluate FSFP considering all the possible variables as first choice and then choosing the best one, but both these methods lead to a huge increase in computational cost. The approach we have chosen instead is to select the first variable using FSCA. The resulting algorithm, denoted as FSFP-FSCA, is given in Algorithm 8.

---

**Algorithm 7** FSFP

---

**Input:**  $\mathbf{X}, k$

- 1:  $I_U = \{1, 2, \dots, v-1, v\}; I_S = \emptyset$
  - 2: **for**  $j = 1$  to  $k$  **do**
  - 3:      $i^* = \operatorname{argmax}_{i \in I_U} \{FP(\mathbf{X}) - FP(\mathbf{X}_{S \cup \{x_i\}})\}$
  - 4:      $I_S = I_S \cup \{i^*\}; I_U = I_U \setminus \{i^*\}$
  - 5: **end for**
  - 6: **return**  $I_S$
- 

### 3.6. Unsupervised Forward Selection (UFS)

Whitley et al. [30] proposed a feature selection method in the context of computational chemistry and drug design, which they refer to as unsupervised forward selection (UFS). The effect of an agent on a biological system can be evaluated through bioassays to capture the responses of process variables to stimuli. The large number of variables involved often makes the identification of relationships among them challenging, therefore UFS has been developed to eliminate feature redundancy by identifying a reduced set of relevant system

---

**Algorithm 8** FSFP-FSCA

---

**Input:**  $\mathbf{X}, k$ 

- 1: Normalize  $\mathbf{X}$  to have unitary norm columns
  - 2:  $I_S = FSCA(\mathbf{X}, 1); I_U = \{1, 2, \dots, v-1, v\} \setminus I_S$
  - 3: **for**  $j = 2$  to  $k$  **do**
  - 4:      $i^* = \operatorname{argmax}_{i \in I_U} \{FP(\mathbf{X}) - FP(\mathbf{X}_{S \cup \{\mathbf{x}_i\}})\}$
  - 5:      $I_S = I_S \cup \{i^*\}; I_U = I_U \setminus \{i^*\}$
  - 6: **end for**
  - 7: **return**  $I_S$
- 

properties. The selection metric employed is the *squared multiple correlation coefficient* with respect to an orthonormal basis spanning the columns of  $\mathbf{X}$  corresponding to the already selected variables,  $\mathbf{X}_S$ , with the orthonormal basis computed by, for example, the Gram-Schmidt procedure. Denoting the orthonormal basis corresponding to  $\mathbf{X}_S$  as  $\mathbf{C}_S = [\mathbf{c}_1, \mathbf{c}_2, \dots, \mathbf{c}_{|I_S|}]$ , the squared multiple correlation coefficient  $R^2$  of vector  $\mathbf{x}_i$ ,  $i \in I_U$ , is defined as

$$R^2(\mathbf{x}_i, \mathbf{C}_S) = \left| \sum_{j=1}^{|I_S|} \mathbf{c}_j^T \mathbf{x}_i \mathbf{c}_j \right|^2 = \sum_{j=1}^{|I_S|} (\mathbf{c}_j^T \mathbf{x}_i)^2 = \mathbf{x}_i^T \mathbf{C}_S \mathbf{C}_S^T \mathbf{x}_i \quad (31)$$

Using this metric the UFS algorithm selects at each iteration the variable with the smallest  $R^2$ , while discarding variables whose  $R^2$  value exceeds a user defined similarity threshold  $R_{max}^2$ , until all variables have either been selected or discarded. To maintain consistency with the forward greedy variable selection algorithm structure considered in this paper (Algorithm 1), in our implementation of UFS we omit the similar variable pruning step and instead terminate when  $k$  variables have been selected, as described in Algorithm 9.

The UFS algorithm is equivalent to defining the selection metric  $g(\cdot)$  in Algorithm 1 as

$$g(I_S) = - \sum_{j=1}^{|I_S|} \sum_{i=1}^{j-1} (\mathbf{c}_i^T \mathbf{x}_j)^2 \quad (32)$$

which corresponds to defining the marginal gain as  $-R^2(\mathbf{x}, \mathbf{C}_{S_k})$  and replacing *argmin* with *argmax* at step 6 of Algorithm 9. It can be shown that this

---

**Algorithm 9** UFS

---

**Input:**  $\mathbf{X}, k$ 

- 1: Normalize  $\mathbf{X}$  to have unitary norm columns
  - 2:  $\mathbf{Q} = \mathbf{X}^T \mathbf{X}$
  - 3:  $I_S = \{i_1, i_2\}$ , where  $i_1$  and  $i_2$  ( $i_1 < i_2$ ) are the row and column indices of the element of  $\mathbf{Q}$  with the smallest absolute value
  - 4: Define an orthonormal basis of the variables indexed by  $I_S : \mathbf{C}_{S_2} = [\mathbf{c}_1, \mathbf{c}_2]$  where  $\mathbf{C}_{S_2} = \text{Gram-Schmidt}(\mathbf{X}_{I_S})$
  - 5: **for**  $j = 3$  to  $k$  **do**
  - 6:      $i^* = \operatorname{argmin}_{i \in I_U} R^2(\mathbf{x}_i, \mathbf{C}_{S_{j-1}})$
  - 7:      $I_S = I_S \cup \{i^*\}; I_U = I_U \setminus \{i^*\}$
  - 8:      $\mathbf{C}_{S_j} = \text{Gram-Schmidt}(\mathbf{X}_{I_S})$
  - 9: **end for**
  - 10: **return**  $I_S$
- 

metric is a submodular function, hence an exact lazy greedy implementation of UFS is possible. However,  $g(I_S)$  is a monotone decreasing function, rather than increasing, and therefore the  $\mathcal{B}_N$  performance bound (Eq. 3) does not apply.

### 3.7. Computational Complexity

All the algorithms considered share a similar greedy selection structure, and all rely on the existence of linear dependency between the selected and unselected variables. The element that distinguishes one algorithm from another is the variable selection criterion employed (see Table 2). The differences in these criteria result in algorithms with substantially different computational complexity, as summarised in Table 3. FSCA and FOS-MOD have the same order of magnitude of computational complexity with the only difference between them being an additional dot product term in the FOS-MOD metric, as discussed in [24]. Whenever computing FSCA or FOS-MOD is prohibitive, PFS can be employed in conjunction with the Nonlinear Iterative Partial Least Squares (NIPALS) algorithm [47] to compute the first principal component, yielding a



$O((4N + 8)kmv) \rightarrow O(Nkmv)$  complexity algorithm [24]. Here  $N$  denotes the average number of iterations for the NIPALS algorithm to converge to the first principle component. The lazy greedy formulation of FSCA achieves a similar complexity to PFS.

The term  $O(mv^2)$  arises in FSFP-FSCA due to the complexity of selecting the first variable using FSCA, whereas in both ITFS and UFS it is associated with the initial computation of the  $v \times v$  covariance matrices,  $\Sigma_{UU}$  and  $\mathbf{Q}$ , respectively. ITFS is dominated by the  $O(v^3)$  inverse covariance calculation which is repeated approximately  $v$  times per iteration and for each of the  $k$  variables selected, hence the  $O(kv^4)$  complexity of this algorithm. A lazy greedy implementation reduces this to  $O(kv^3)$  [9]. In the FSFP-FSCA and UFS algorithms the FP and  $R^2$  variable selection metrics have  $O(j^2mv)$  and  $O(jmv)$  complexity, respectively, at the  $j$ -th iteration, hence the accumulated complexity for these operations over  $k$  iterations is  $O(k^3mv)$  and  $O(k^2mv)$ , respectively. Since FP is submodular, a lazy implementation of FSFP-FSCA has complexity  $O(mv^2 + k^3m)$  as the first selection performed via FSCA requires  $O(mv^2)$  and the subsequent iterations require  $O(k^3m)$ . Similarly, UFS has an  $O(mv^2 + k^2m)$  lazy implementation. The formulation of the PFS algorithm is not compatible with a lazy implementation. Also, a greedy implementation of the non-submodular FOS-MOD algorithm has not been reported in the literature and its feasibility has not been investigated in this work, hence it is recorded as “not investigated” in the table.

#### 4. Results

This section compares the performance of the algorithms described above, namely FSCA, L-FSCA, FOS-MOD, PFS, ITFS, FSFP-FSCA and UFS, on simulated and real world datasets taken from the UCI Machine Learning Repository and provided by a semiconductor manufacturer. For reasons of space, in this section FOS-MOD will be referred to as FOS, FSFP-FSCA as FP-CA and L-FSCA as L-CA.

Table 2: The selection criterion corresponding to each considered algorithm.

Method name	Selection criterion for $i \in I_U \rightarrow I_S$
FSCA [24]	Max. explained variance with respect to $\mathbf{X}$ (or $\mathbf{R}$ )
L-FSCA	Max. explained variance with respect to $\mathbf{X}$ (or $\mathbf{R}$ )
PFS [23]	Max. correlation with the first PC of the residual matrix $\mathbf{R}$
FOS-MOD [29]	Max. squared correlation with respect to $\mathbf{X}$ (or $\mathbf{R}$ )
FSFP-FSCA	Min. frame potential of the selected variables $\mathbf{X}_S$
ITFS [9]	Max. mutual information between $\mathbf{X}_S$ and $\mathbf{X}_U$
UFS [30]	Min. correlation with the selected variables $\mathbf{X}_S$

Table 3: Computational complexity of the variable selection methods under consideration (when selecting  $k$  variables):  $k$  is the number of selected variables,  $v$  is the number of candidate variables,  $m$  is the number of measurements (observations) and  $N$  is the mean number of iterations for the PCA algorithm to converge to the first principal component in PFS.

Algorithm	Complexity ( $k \ll v$ )	Lazy Implementation
FSCA	$O(kmv^2)$	$\rightarrow O(kmv)$
FOS-MOD	$O(kmv^2)$	not investigated
PFS (NIPALS)	$O(Nkmv)$	not applicable
ITFS	$O(mv^2 + kv^4)$	$\rightarrow O(mv^2 + kv^3)$
FSFP-FSCA	$O(mv^2 + k^3mv)$	$\rightarrow O(mv^2 + k^3m)$
UFS	$O(mv^2 + k^2mv)$	$\rightarrow O(mv^2 + k^2m)$

The comparison is based on six metrics. Three of these are the variance explained  $V_{\mathbf{X}}(\mathbf{X}_S)$ , the frame potential  $FP(\mathbf{X}_S)$  and the mutual information  $MI(\mathbf{X}_S)$ , as previously defined in Eq. (16), (29) and (25), respectively. These are complemented by three metrics introduced to characterise the evolution of  $V_{\mathbf{X}}(\mathbf{X}_S)$  with the number of selected variables  $k$ , namely, the area under the variance curve  $AUC$ , the relative performance  $r$ , and the number of variables needed to reach  $n\%$  variance explained  $k_{n\%}$ .  $AUC$  is defined as

$$AUC = \frac{0.01}{v-1} \sum_{k=1}^{v-1} V_{\mathbf{X}}(\hat{\mathbf{X}}_k) \quad (33)$$

where  $\hat{\mathbf{X}}_k$  denotes the approximation of  $\mathbf{X}$  with  $\mathbf{X}_S$ , where  $|I_S| = k$ , as defined in Eq. (18). The factor  $100(v-1)$  normalises the expression to yield a maximum value of 1 when 100% of the variance is explained by a single variable. The relative performance  $r$  expresses how well an algorithm performs relative to the other algorithms over the first  $k_{99\%}^*$  selected variables. Specifically, it is the percentage of times over the interval  $k = 1, \dots, k_{99\%}^*$  that the algorithm is the top ranked, i.e. yields the maximum value of  $V_{\mathbf{X}}(\hat{\mathbf{X}}_k)$ , that is,

$$r = \frac{100}{k_{99\%}^*} \sum_{k=1}^{k_{99\%}^*} is\_top\_rank(k). \quad (34)$$

Here  $k_{99\%}^*$  denotes the minimum value of  $k$  required to have all the algorithms exceeding 99% variance explained and  $is\_top\_rank(k)$  is 1 if the algorithm is the best among those being evaluated and zero otherwise, for  $|I_S| = k$ . Finally,  $k_{n\%}$  provides a measure of the level of compression provided for a given target reconstruction accuracy  $n$ , and is defined as

$$k_{n\%} = \underset{k}{\operatorname{argmin}} V_{\mathbf{X}}(\hat{\mathbf{X}}_k) \quad s.t. \quad V_{\mathbf{X}}(\hat{\mathbf{X}}_k) \geq n. \quad (35)$$

Note that the  $AUC$ ,  $r$  and  $k_{n\%}$  metrics are functions of VE, hence algorithms optimizing VE are implicitly optimizing them too. The choice of having four out of six metrics based on VE is motivated by the fact that, in contrast to MI and FP, VE is a direct measurement of the approximation error  $\mathbf{X} - \hat{\mathbf{X}}$  which, in practice, is the quantity we wish to minimize.

Table 4: Overview of the case study datasets.

Dataset	$m$	$v$
Simulated 1 [24]	1000	26
Simulated 2 [24]	1000	50
Pitprops	180	13
Semiconductor	316	50
Arrhythmia <sup>1</sup>	452	258
Sales <sup>2</sup>	812	52
Gases <sup>3</sup>	1586	129
Music <sup>4</sup>	1059	68

<sup>1</sup> <https://archive.ics.uci.edu/ml/datasets/Arrhythmia><sup>2</sup> [https://archive.ics.uci.edu/ml/datasets/Sales\\_Transactions\\_Dataset\\_Weekly](https://archive.ics.uci.edu/ml/datasets/Sales_Transactions_Dataset_Weekly)<sup>3</sup> <https://archive.ics.uci.edu/ml/datasets/Gas+Sensor+Array+Drift+Dataset+at+Different+Concentrations><sup>4</sup> <https://archive.ics.uci.edu/ml/datasets/Geographical+Original+of+Music>

Table 4 lists the datasets considered in our comparative study. The code for this paper is written in MATLAB and is publicly available<sup>4</sup> to facilitate further benchmarking of greedy search algorithms for unsupervised variable selection. Our results are achieved using MATLAB R2020a.

#### 4.1. Preliminary Overview

Table 5 gives a preliminary overview of the performance of the algorithms on each dataset. The metrics reported are the  $AUC$  and the  $k_n\%$  with  $n \in \{95, 99\}$ .  $k_n\%$  suggests that FSCA and its lazy version provide the highest level of compression in all datasets with the exception of  $k_{95\%}$  in ‘Music’ and ‘Simulated 1’. The lazy version of FSCA achieves the same performance as FSCA on all eight datasets, confirming that, while VE is not submodular, it

<sup>4</sup><https://github.com/fedezocco/GreedyVarSel-MATLAB>

essentially behaves in a submodular fashion with respect to greedy selection. An inspection of the sequence of variables selected by each algorithm showed that small deviations did occur with L-FSCA for the ‘Sales’, ‘Arrhythmia’ and ‘Pitprops’ datasets. It produced a different permutation in the sequence of selected variables between  $k = 9$  and  $k = 30$  with ‘Sales’ and between  $k = 25$  and  $k = 29$  with ‘Arrhythmia’. This resulted in a maximum VE deviation of 0.006 within these intervals, but no deviation thereafter. In the ‘Pitprops’ dataset L-FSCA selected a different variable at  $k = 10$  resulting in a reduction in VE of 0.006 at that point. However, the net impact when the 11th variable is included is a positive deviation (increase in VE) of 0.04 (see Table 8). FSCA methods show 13 values of  $k_n\%$  in bold, followed by PFS with 12, ITFS with 8, FOS with 6, FP-CA with 3 and UFS with 0. The area under the VE curve, i.e.  $AUC$ , is greatest with FSCA methods for 6 datasets, followed by PFS with 5, FOS with 2 and 0 for the remaining algorithms. ‘Pitprops’ and ‘Music’ are the datasets most difficult to compress to a lower dimension as they provide the lowest values of  $AUC$  (0.756 and 0.785, respectively). In contrast, despite having the second highest dimension  $v$ , ‘Gases’ can be represented by just 3 variables with 99% accuracy.

The indices of the variables selected by each algorithm for selected datasets are shown in Table 6. Each table entry is the index of the variable selected at the  $k$ -th iteration. The sequence of variables selected by a given algorithm is therefore defined by the corresponding table column. In all cases FSCA and its lazy implementation L-CA select the same variables which further sustains the hypothesis that variance explained is behaving as a submodular function with these datasets. The frame-potential-based algorithm, i.e. FP-CA, selects the same first variable as FSCA because, as discussed in the previous section, FSCA is used for  $k = 1$  before switching to a FP-based selection when  $k > 1$ . The FP-based selection overall does not show similarities with MI-based and VE-based selections. In ‘Simulated 1’ PFS, FSCA, L-CA, ITFS and FOS select the same set when  $k = 6$ , but the variables are selected with a different order. In ‘Sales’, five out of the six variables selected by ITFS are in common with

Table 5: (All datasets) A summary of the performance of the different selection algorithms. Best values are in bold.

Dataset	Metric	FSCA	L-CA	FP-CA	PFS	ITFS	FOS	UFS	$v$
Semic.	$k_{95\%}$	<b>4</b>	<b>4</b>	6	<b>4</b>	<b>4</b>	<b>4</b>	5	
	$k_{99\%}$	<b>7</b>	<b>7</b>	10	<b>7</b>	<b>7</b>	<b>7</b>	9	50
	$AUC$	<b>0.976</b>	<b>0.976</b>	0.969	<b>0.976</b>	0.970	0.975	0.961	
Pitpr.	$k_{95\%}$	<b>9</b>	<b>9</b>	<b>9</b>	<b>9</b>	<b>9</b>	<b>9</b>	10	
	$k_{99\%}$	11	11	11	11	11	11	11	13
	$AUC$	<b>0.756</b>	<b>0.756</b>	0.726	<b>0.756</b>	0.730	<b>0.756</b>	0.683	
Arryt.	$k_{95\%}$	<b>47</b>	<b>47</b>	241	<b>47</b>	144	178	193	
	$k_{99\%}$	<b>71</b>	<b>71</b>	256	<b>71</b>	173	240	239	258
	$AUC$	<b>0.954</b>	<b>0.954</b>	0.688	0.952	0.844	0.849	0.741	
Sales	$k_{95\%}$	<b>5</b>	<b>5</b>	7	<b>5</b>	<b>5</b>	9	13	
	$k_{99\%}$	<b>38</b>	<b>38</b>	41	39	40	42	42	52
	$AUC$	<b>0.976</b>	<b>0.976</b>	0.975	<b>0.976</b>	0.975	0.970	0.968	
Gases	$k_{95\%}$	<b>2</b>	<b>2</b>	<b>2</b>	<b>2</b>	<b>2</b>	3	4	
	$k_{99\%}$	<b>3</b>	<b>3</b>	6	<b>3</b>	11	9	17	129
	$AUC$	<b>0.999</b>	<b>0.999</b>	0.998	<b>0.999</b>	0.992	0.991	0.988	
Music	$k_{95\%}$	49	49	53	<b>48</b>	49	49	56	
	$k_{99\%}$	<b>61</b>	<b>61</b>	64	<b>61</b>	<b>61</b>	<b>61</b>	64	68
	$AUC$	0.785	0.785	0.758	<b>0.786</b>	0.771	0.785	0.724	
Sim. 1	$k_{95\%}$	5	5	<b>4</b>	5	<b>4</b>	<b>4</b>	15	
	$k_{99\%}$	<b>6</b>	<b>6</b>	7	<b>6</b>	<b>6</b>	<b>6</b>	21	26
	$AUC$	0.935	0.935	0.935	0.935	0.934	<b>0.937</b>	0.779	
Sim. 2	$k_{95\%}$	<b>18</b>	<b>18</b>	24	19	23	19	25	
	$k_{99\%}$	<b>22</b>	<b>22</b>	25	<b>22</b>	25	23	25	50
	$AUC$	<b>0.863</b>	<b>0.863</b>	0.770	0.855	0.812	0.852	0.750	

FSCA/L-CA. Moreover, for  $k = 6$ , UFS has five variables in common with FOS and FP-CA. In ‘Simulated 2’ and ‘Semiconductor’: the only relevant similarity among the algorithm selections is in the latter, where FSCA/L-CA and PFS share three variables when  $k = 5$ .

#### 4.2. Simulated Datasets

**Simulated dataset 1.** In this dataset, which is from [24], a set of 4 i.i.d. variables  $w, x, y, z \sim \mathcal{N}(0, 1)$  and 22 noise variables,  $\epsilon_i \sim \mathcal{N}(0, 0.1)$ ,  $i = 1, \dots, 20$  and  $\epsilon_{21}, \epsilon_{22} \sim \mathcal{N}(0, 0.4)$  are used to create a set of dependent variables  $w_i = w + \epsilon_i$ ,  $x_i = x + \epsilon_{i+5}$ ,  $y_i = y + \epsilon_{i+10}$ ,  $z_i = z + \epsilon_{i+15}$ , for  $i = 1, \dots, 5$ , and  $h_1 = w + x + \epsilon_{21}$ ,  $h_2 = y + z + \epsilon_{22}$ . The final matrix is then defined as

$$\mathbf{X} = [\mathbf{w}, \mathbf{w}_1, \dots, \mathbf{w}_5, \mathbf{x}, \mathbf{x}_1, \dots, \mathbf{x}_5, \mathbf{y}, \mathbf{y}_1, \dots, \mathbf{y}_5, \mathbf{z}, \mathbf{z}_1, \dots, \mathbf{z}_5, \mathbf{h}_1, \mathbf{h}_2] \quad (36)$$

with the columns generated as  $m = 1000$  realizations of the random variables, yielding a dataset  $\mathbf{X} \in \mathbb{R}^{1000 \times 26}$ .

Figure 3 shows the explained variance as a function of the number of selected variables for each algorithm. With the exception of UFS, all the methods achieve a VE greater than 90% with 4 variables. Recalling Table 5, in this case FOS is the best according to all three metrics, whereas UFS requires more than 6 variables to exceed 95% VE, which is beyond the figure horizontal axis limit. As observed in Table 6, in this dataset the algorithms select similar variable sequences with the exception of UFS.

**Simulated dataset 2.** This dataset is also taken from [24] and is characterized by having two blocks of variables. The first block  $\mathbf{X}^I$  is composed of  $u$  independent variables, while the second block  $\mathbf{X}^D$  is linearly dependent on the first block and is obtained as a random linear combination of the variables in  $\mathbf{X}^I$  perturbed by additive Gaussian noise. More formally, the dataset is defined as follows:

- $\mathbf{X}^I \in \mathbb{R}^{m \times u} : \mathbf{X}_{i,j}^I \sim \mathcal{N}(0, 1)$
- $\mathbf{X}^D \in \mathbb{R}^{m \times (v-u)} : \mathbf{X}^D = \mathbf{X}^I \Phi + \mathcal{E}$

Table 6: (Multiple datasets) Ordered indices of the selected variables for four datasets and for  $k = 1, \dots, 6$ . For each value of  $k$ , the  $k$ -th selected variable is indicated.

Dataset	$k$	FSCA	L-CA	FP-CA	PFS	ITFS	FOS	UFS
Sim. 1	1	{26}	{26}	{26}	{25}	{1}	{25}	{26}
	2	{25}	{25}	{1}	{26}	{13}	{13}	{1}
	3	{19}	{19}	{9}	{19}	{7}	{19}	{5}
	4	{1}	{1}	{22}	{1}	{19}	{1}	{2}
	5	{7}	{7}	{17}	{7}	{25}	{7}	{6}
	6	{13}	{13}	{25}	{13}	{26}	{26}	{4}
Sim. 2	1	{49}	{49}	{49}	{38}	{49}	{34}	{22}
	2	{35}	{35}	{25}	{35}	{19}	{28}	{6}
	3	{29}	{29}	{10}	{37}	{29}	{31}	{11}
	4	{31}	{31}	{18}	{49}	{12}	{43}	{21}
	5	{45}	{45}	{8}	{36}	{1}	{26}	{24}
	6	{27}	{27}	{19}	{39}	{16}	{47}	{7}
Semic.	1	{45}	{45}	{45}	{45}	{35}	{42}	{14}
	2	{27}	{27}	{14}	{27}	{15}	{27}	{12}
	3	{1}	{1}	{11}	{23}	{25}	{1}	{5}
	4	{24}	{24}	{4}	{21}	{46}	{21}	{24}
	5	{9}	{9}	{1}	{9}	{31}	{38}	{49}
	6	{49}	{49}	{9}	{16}	{16}	{46}	{26}
Sales	1	{48}	{48}	{48}	{48}	{48}	{42}	{48}
	2	{38}	{38}	{1}	{38}	{9}	{1}	{1}
	3	{9}	{9}	{2}	{17}	{49}	{4}	{2}
	4	{52}	{52}	{52}	{51}	{52}	{2}	{3}
	5	{17}	{17}	{3}	{9}	{17}	{3}	{4}
	6	{49}	{49}	{4}	{43}	{45}	{5}	{5}



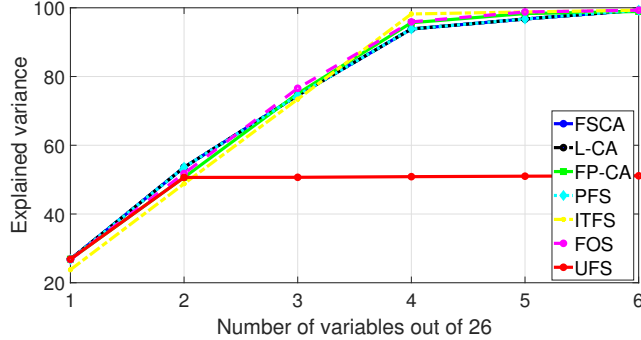


Figure 3: (Simulated 1) Variance explained as a function of the number of selected variables  $k$ .

- $\mathbf{X} \in \mathbb{R}^{m \times v} : \mathbf{X} = [\mathbf{X}^I \ \mathbf{X}^D]$

The matrices  $\Phi \in \mathbb{R}^{u \times (v-u)}$  and  $\mathcal{E} \in \mathbb{R}^{m \times (v-u)}$  can be generated by sampling each element from a Gaussian distribution, in particular  $\Phi_{i,j} \sim \mathcal{N}(0, 1)$  and  $\mathcal{E}_{i,j} \sim \mathcal{N}(0, 0.1)$ . The algorithms were evaluated for the case  $u = 25$ ,  $v = 50$  and  $m = 1000$ .

Table 7 reports the values of VE, MI and FP of each algorithm for  $k = 5, 10$ . All three metrics increase with  $k$ . For  $k = 5$  the best value of each metric is achieved by the algorithm designed to optimize it, that is, VE, MI and FP achieve their best results with FSCA/L-CA, ITFS and FP-CA, respectively. For  $k = 10$  this pattern is broken for FP, with UFS yielding the lowest FP, although FP-CA is a close second. It is also noteworthy that UFS achieves the same FP as FP-CA for  $k = 5$ . This is simply a reflection of the fact that, like FP, the UFS selection process encourages orthogonality among the selected variables. PFS and FOS rank second and third in terms of VE as their selection criterion is related to variance explained. The second best methods in terms of MI are the ones optimizing VE, i.e. FSCA and L-CA. According to Table 5, in this dataset the best methods in terms of  $k_n\%$  and  $AUC$  are FSCA and L-CA followed closely by PFS and FOS.

Table 7: (Simulated 2) Comparison of the VE, FP and MI values obtained with each algorithm. Best results are highlighted in bold.

$ I_S $	Algorithm	Variance Explained	Frame Potential	Mutual Information
$k = 5$	FSCA	<b>43.32</b>	5.26	63.21
	L-CA	<b>43.32</b>	5.26	63.21
	FP-CA	23.70	<b>5.02</b>	62.06
	PFS	39.99	6.01	62.66
	ITFS	36.18	5.21	<b>63.70</b>
	FOS	39.64	6.01	61.22
	UFS	19.30	<b>5.02</b>	27.82
$k = 10$	FSCA	<b>71.08</b>	12.64	90.62
	L-CA	<b>71.08</b>	12.64	90.62
	FP-CA	42.22	10.22	89.05
	PFS	68.58	12.94	90.04
	ITFS	56.88	10.96	<b>91.57</b>
	FOS	68.45	14.19	88.59
	UFS	37.56	<b>10.07</b>	54.55

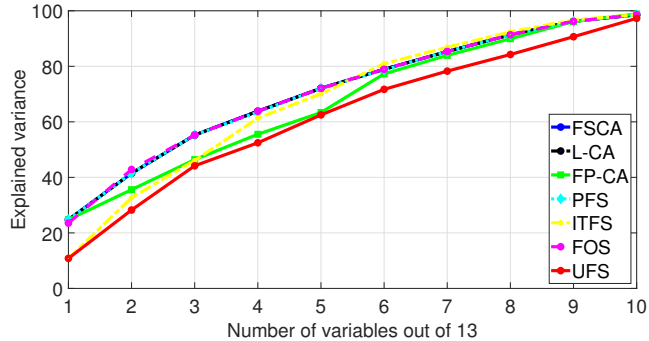


Figure 4: (Pitprops) Variance explained as a function of the number of selected variables  $k$ .

#### 4.3. Pitprops Dataset

The ‘Pitprops’ dataset was first introduced by [48] for PCA performance analysis. The data are measurements of physical properties taken from different species of pit props. The scope of that analysis was to determine if the considered pit props were sufficiently strong for deployment in mines. The considered population included samples of different species, size and geographical region. In [48] the correlation matrix of the original dataset is provided. An approximation of the original 13 attributes is then defined in order to obtain a correlation matrix close to the original one, yielding a data matrix  $\mathbf{X} \in \mathbb{R}^{180 \times 13}$ . The small size of  $v$  in this dataset permits an exhaustive search to be performed for the optimal subset of variables for a fixed value of  $k$ .

As Fig. 4 shows, all the algorithms have similar performance in this case study with the greatest difference visible for  $k \leq 5$ , where UFS, FP-CA and ITFS are the worst performing methods. The similarity of the methods is confirmed by Table 5 with  $9 \leq k_{n\%} \leq 11$  and  $0.683 \leq AUC \leq 0.756$ .

Table 8 details the variance explained by each method with increasing  $k$ , and their relative performance  $r$ . The corresponding PCA values are reported for comparison. ITFS shows a particular trend. For  $k \leq 5$  it is worse than FSCA, L-CA and FOS, while for  $k > 5$  it is the best method. Hence, overall, ITFS has the highest  $r$ . The highest  $AUC$  of 0.756 is obtained with FSCA, L-CA, PFS

Table 8: (Pitprops) The explained variance  $V_{\mathbf{X}}(\hat{\mathbf{X}}_k)$  by each algorithm for different values of  $k$ . The relative performance ( $r$ ) and  $AUC$  metrics are reported at the bottom. The best methods after PCA for each value of  $k$  are highlighted in bold.

$k$	PCA	FSCA	L-CA	FP-CA	PFS	ITFS	FOS	UFS
1	30.39	<b>24.76</b>	<b>24.76</b>	<b>24.76</b>	<b>24.76</b>	10.82	23.53	10.82
2	49.88	41.48	41.48	35.56	41.48	32.65	<b>42.84</b>	28.24
3	62.60	<b>55.24</b>	<b>55.24</b>	46.4	<b>55.24</b>	46.09	<b>55.24</b>	44.17
4	71.31	<b>63.82</b>	<b>63.82</b>	55.51	63.49	61.33	<b>63.82</b>	52.45
5	78.98	<b>72.08</b>	<b>72.08</b>	63.37	<b>72.08</b>	70.07	<b>72.08</b>	62.50
6	85.83	78.93	78.93	77.27	78.72	<b>80.94</b>	78.93	71.70
7	91.57	85.34	85.34	83.94	85.34	<b>86.88</b>	85.34	78.27
8	95.50	91.36	91.36	89.93	91.36	<b>92.39</b>	91.36	84.25
9	98.14	96.21	96.21	96.12	96.21	<b>96.76</b>	96.21	90.66
10	99.41	98.57	98.56	<b>98.85</b>	98.57	98.56	98.57	97.28
11	99.74	99.41	99.45	99.43	99.41	<b>99.46</b>	99.41	99.41
$r$	-	36.4	36.4	18.2	27.3	<b>45.5</b>	36.4	0
$AUC$	0.803	<b>0.756</b>	<b>0.756</b>	0.726	<b>0.756</b>	0.730	<b>0.756</b>	0.683

and FOS followed by ITFS with 0.730.

Table 9 lists the variables selected at each step by each algorithm and compares them with the optimal solution for  $|I_S| = 7$ . The number of selected variables that each method has in common with the optimal solution is expressed as the parameter  $n_b$  in the final row of the table (i.e.  $n_b = |I_S^* \cap I_S|$ ). ITFS finds the optimum solution. The next closest are UFS with  $n_b = 5$  and FP-CA with  $n_b = 4$ . ITFS also yields the highest VE. FSCA, L-CA, PFS and FOS only have 3 variables in common with the optimum subset, but in terms of VE they give the second highest value (85.3%) followed by FP-CA (83.9%) and UFS (78.3%). FSCA/L-CA and FOS select the same seven features, but ‘length’ and ‘ringbut’ are selected as first and third variables, respectively, by FSCA/L-CA, whereas FOS selects them as third and first variables, respectively. Similarly,

Table 9: (Pitprops) First 7 variables selected by each algorithm compared with the optimal subset with respect to VE. The order in which the variables are listed reflects the order of their greedy selection. The parameter  $n_b$  is the number of selected variables each algorithm has in common with the optimal subset. The best values are highlighted in bold.

best	FSCA	L-CA	FP-CA	PFS	ITFS	FOS	UFS
topdiam	length	length	length	length	knots	ringbut	knots
testsg	moist	moist	knots	moist	topdiam	moist	bowdist
ringbut	ringbut	ringbut	diaknot	ringbut	testsg	length	length
bowdist	clear	clear	clear	bowmax	ringbut	clear	topdiam
clear	bowmax	bowmax	ovensg	clear	clear	bowmax	ringtop
knots	ovensg	ovensg	testsg	knots	bowdist	ovensg	clear
diaknot	knots	knots	bowmax	ovensg	diaknot	knots	diaknot
Variance explained							
86.9	85.3	85.3	83.9	85.3	<b>86.9</b>	85.3	78.3
Number of optimal variables selected ( $n_b$ )							
-	3	3	4	3	<b>7</b>	3	5

PFS selects the same variables, but in a different order. Consequently, the VE at  $k = 7$  for FSCA, L-CA, FOS and PFS is the same. The fact that these four methods achieve a VE that is 98% of the optimum solution with  $n_b = 3$ , while UFS only achieves a VE that is 90% of the optimum with  $n_b = 5$ , highlights how the complex correlation relationships between variables makes optimum variable selection such a challenging problem.

#### 4.4. Wafer Profile Reconstruction

This case study was provided by a semiconductor manufacturer and is concerned with determining a reduced and optimal set of measurement sites distributed over a silicon wafer surface in order to adequately monitor the uniformity of the thickness of a layer of material being deposited by a chemical vapour deposition production process. The dataset consists of measurements taken at 50 candidate sites from a set of 316 wafers, hence  $\mathbf{X} \in \mathbb{R}^{316 \times 50}$ . As

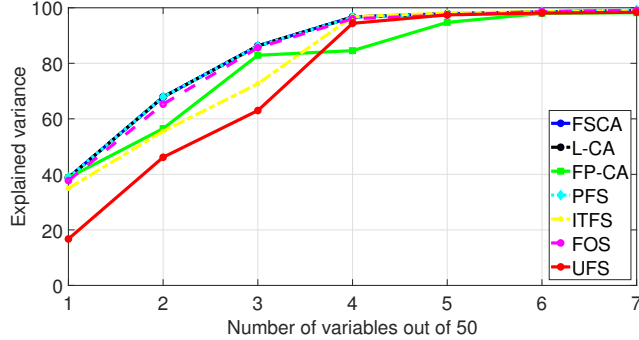


Figure 5: (Semiconductor) Variance explained as a function of the number of selected variables  $k$ .

process monitoring is a time consuming activity, it is desirable to have a reduced set of measurement sites while at the same time maintaining an accurate representation of the surface variation [10, 44].

The surface monitoring accuracy and the number of measurement sites are expressed through the variance explained and the number of selected sites  $k$ , respectively. The comparison of the candidate algorithms is shown in Fig. 5. While for  $k \geq 5$  the methods are equivalent, for  $k < 5$  FSCA, L-CA, ITFS and PFS provide the highest VE. The VE values with increasing  $k$  are reported in Table 10. While PCA requires 5 components to exceed 99%, the greedy feature selection algorithms require from a minimum of 7 variables with FSCA, L-CA, PFS, ITFS and FOS to a maximum of 10 with FP-CA. The highest relative performance  $r$  is 60% and is achieved by FSCA and L-CA; ITFS ranks second with 40%. The  $AUC$  values are all similar with just a difference of 0.015 between the highest and the lowest, which indicates that, overall, all the candidate algorithms have a similar trend in terms of VE.

The values of VE, FP and MI obtained with each variable selection algorithm are compared in Table 11 for  $k = 3, 7$ . All the three metrics increase with  $k$ . While the best values of FP and MI are achieved by the corresponding algorithms, the best value of VE for  $k = 7$  is given by PFS, followed by FOS and then ITFS. This contrasts with the results for  $k = 3$  and the results for the

Table 10: (Semiconductor) Number of selected sites  $k$  and the corresponding explained variance  $V_{\mathbf{X}}(\hat{\mathbf{X}}_k)$  for each algorithm. The relative performance ( $r$ ) and  $AUC$  metrics are reported at the bottom. The best values after PCA for each  $k$  are highlighted in bold.

$k$	PCA	FSCA	L-CA	FP-CA	PFS	ITFS	FOS	UFS
1	41.05	<b>38.81</b>	<b>38.81</b>	<b>38.81</b>	<b>38.81</b>	35.00	37.76	16.74
2	70.19	<b>67.86</b>	<b>67.86</b>	56.50	<b>67.86</b>	55.52	65.28	46.16
3	88.35	<b>86.28</b>	<b>86.28</b>	82.90	86.25	72.64	85.59	62.99
4	98.47	96.68	96.68	84.56	96.62	<b>96.77</b>	96.07	94.41
5	99.08	97.87	97.87	94.75	97.77	<b>98.15</b>	97.37	97.45
6	99.43	98.53	98.53	97.98	98.61	<b>98.63</b>	98.62	98.10
7	99.64	99.02	99.02	98.22	<b>99.18</b>	99.06	99.10	98.40
8	99.72	<b>99.42</b>	<b>99.42</b>	98.57	99.37	<b>99.42</b>	99.35	98.88
9	99.79	<b>99.60</b>	<b>99.60</b>	98.76	99.54	99.58	99.59	99.30
10	99.85	<b>99.69</b>	<b>99.69</b>	99.14	99.65	99.66	99.67	99.40
$r$	-	<b>60</b>	<b>60</b>	10	30	40	0	0
$AUC$	0.979	<b>0.976</b>	<b>0.976</b>	0.969	<b>0.976</b>	0.970	0.975	0.961

Table 11: (Semiconductor) Comparison of the VE, FP and MI values obtained with each variable selection algorithm. Best results are highlighted in bold.

$ I_S $	Algorithm	Variance	Frame	Mutual
		Explained	Potential	Information
$k = 3$	FSCA	<b>86.28</b>	8.998	96.95
	L-CA	<b>86.28</b>	8.998	96.95
	FP-CA	82.90	<b>8.997</b>	93.25
	PFS	86.25	8.998	97.78
	ITFS	72.64	8.998	<b>97.82</b>
	FOS	85.59	8.998	96.22
	UFS	62.99	8.997	17.41
$k = 7$	FSCA	99.02	48.982	113.30
	L-CA	99.02	48.982	113.30
	FP-CA	98.22	<b>48.979</b>	109.87
	PFS	<b>99.18</b>	48.987	114.17
	ITFS	99.06	48.987	<b>115.70</b>
	FOS	99.10	48.987	115.31
	UFS	98.40	48.985	35.68

‘Simulated 2’ dataset reported in Table 7, and is a consequence of the high level of redundancy in this dataset with several combinations of 7 variables sufficient to achieve 99% VE, as evident from Table 6. This is also reflected in the almost identical FP values achieved by all algorithms. For  $k = 3$ , the second ranked algorithm in terms of FP is UFS and in terms of MI it is PFS, while for  $k = 7$  it is FSCA/L-CA and FOS, respectively. Therefore we can see that the algorithms rank quite differently for different metrics, although the overall pattern remains with VE based algorithms performing well in terms of MI, and UFS and FP-CA performing similarly well for FP, but poorly for the other metrics.



#### 4.5. Case studies from the UCI Repository

This section considers four datasets taken from the UCI Machine Learning Repository. The datasets are listed and briefly described below.

**Arrhythmia [49].** This dataset is taken from medical records of arrhythmia patients. It was originally intended to train a classifier able to distinguish between 16 different classes of Arrhythmia defined considering  $m = 452$  patients. The  $v = 279$  features are both identifiers of the particular patient, e.g. age, sex, weight, and sampled electrocardiogram signal recordings. Since there are some missing values present in the original dataset, we have reduced the number of variables to  $v = 258$ . In this scenario, the output of the algorithms  $I_S$  can be interpreted as a reduced set of patient data enabling a faster data collection and training process with regard to the classifier development. Additional information on the dataset can be found in [49].

**Sales [50].** This dataset is composed of weekly purchase quantities of  $m = 811$  products over  $v = 52$  weeks. The data has a time evolution of 52 weeks and the objective is to identify which weeks to record to get the most accurate prediction of the purchases over the other weeks. For a more detailed dataset description the reader should refer to [51].

**Gases [52], [53].** This dataset, which was also considered in our previous work [33], consists of measurements of 8 gas-related parameters provided by each of 16 chemical sensors used to monitor gas level concentrations. Here we considered just the third batch of data, hence  $\mathbf{X} \in \mathbb{R}^{1586 \times 129}$ .

**Music [54].** A set of  $m = 1059$  musical tracks from different countries, each one  $v = 68$  samples long, leads to the final dataset  $\mathbf{X} \in \mathbb{R}^{1059 \times 68}$ . Here variable selection identifies a reduced set of samples/columns, each one corresponding to a specific time within the musical tracks. Refer to [54] for further details.

The results for the UCI case studies are summarized in Table 12 for four different compression thresholds  $k_n\%$ . The best performing algorithm is highlighted in bold in each case. Overall, FSCA/L-CA achieves the highest com-

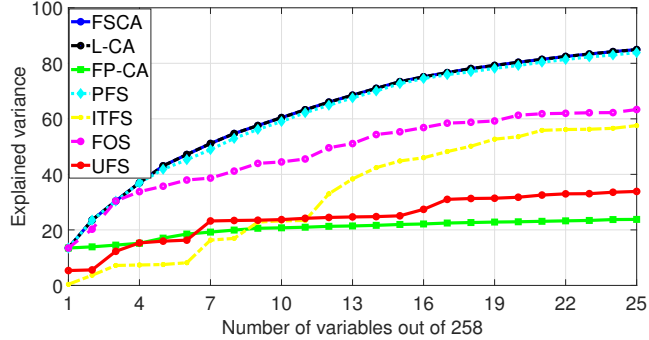


Figure 6: (Arrhythmia) Variance explained as a function of the number of selected variables  $k$ .

pression performance with 12 entries in bold followed by PFS with 9, and then FOS and ITFS with 3 each. The ‘Music’ dataset is the most difficult to compress; for a reconstruction accuracy of 80% the number of samples to record is reduced by 59% with the best algorithm, but it is only reduced by 29% when the desired reconstruction accuracy is 95%. ‘Sales’ only requires a large number of variables at the 99% accuracy level. For lower threshold levels, data from fewer than 10% of the weeks is sufficient to predict the purchases for the remaining weeks using FSCA, L-CA, PFS or ITFS. In the case of ‘Arrhythmia’ the best performing algorithm achieves a 72% reduction in the number of variables to reach 99% reconstruction accuracy, while in the case of ‘Gases’ the reduction is a remarkable 97%.

Figure 6 shows the variance explained as a function of  $k$  with the ‘Arrhythmia’ dataset. There is a significant difference between the best performing methods (FSCA, L-CA and PFS) and the worst ones (UFS, FP-CA and ITFS) for this dataset. Table 12 indicates that similar performance differences are valid also for  $k > 25$ : for example, UFS and FP-CA have  $k_{90\%} > 150$  and  $k_{95\%} > 190$  while the best performing methods have  $k_{90\%} < k_{95\%} < 50$ . FOS gives an intermediate accuracy level for the range of  $k$  values considered in the figure, i.e.  $1 \leq k \leq 25$ , but is overtaken by ITFS for higher values of  $k$ .

Table 12: (UCI datasets) Variable selection algorithm performance on selected UCI benchmark datasets. Four metrics are presented for each algorithm:  $k_{80\%}$ ,  $k_{90\%}$ ,  $k_{95\%}$  and  $k_{99\%}$ . Best values are in bold.

Dataset	$k_n\%$	FSCA	L-CA	FP-CA	PFS	ITFS	FOS	UFS	$v$
Arrhyt.	$k_{80\%}$	<b>20</b>	<b>20</b>	140	21	78	68	119	258
	$k_{90\%}$	<b>33</b>	<b>33</b>	190	34	118	122	153	
	$k_{95\%}$	<b>47</b>	<b>47</b>	241	<b>47</b>	144	178	193	
	$k_{99\%}$	<b>71</b>	<b>71</b>	256	<b>71</b>	173	240	239	
Sales	$k_{80\%}$	1	1	1	1	1	1	1	52
	$k_{90\%}$	1	1	1	1	1	1	1	
	$k_{95\%}$	<b>5</b>	<b>5</b>	7	<b>5</b>	<b>5</b>	9	13	
	$k_{99\%}$	<b>38</b>	<b>38</b>	41	39	40	42	42	
Gases	$k_{80\%}$	<b>1</b>	<b>1</b>	<b>1</b>	<b>1</b>	2	2	2	129
	$k_{90\%}$	2	2	2	2	2	2	2	
	$k_{95\%}$	<b>2</b>	<b>2</b>	<b>2</b>	<b>2</b>	<b>2</b>	3	4	
	$k_{99\%}$	<b>3</b>	<b>3</b>	6	<b>3</b>	11	9	17	
Music	$k_{80\%}$	<b>28</b>	<b>28</b>	29	29	31	<b>28</b>	39	68
	$k_{90\%}$	<b>40</b>	<b>40</b>	42	<b>40</b>	41	<b>40</b>	49	
	$k_{95\%}$	49	49	53	<b>48</b>	49	49	56	
	$k_{99\%}$	<b>61</b>	<b>61</b>	64	<b>61</b>	<b>61</b>	<b>61</b>	64	

## 5. Conclusions

This paper has compared seven *greedy unsupervised* variable selection algorithms, five of which, FSCA, PFS, ITFS, FOS-MOD and UFS, are taken from the literature and two, L-FSCA and FSFP-FSCA, have been proposed for the first time. The comparison is based on six metrics and considers two simulated datasets and six real case studies.

The experimental results show that, with respect to the VE performance metric, the algorithms based on variance explained or the closely related squared correlation selection functions substantially outperform the mutual information based algorithm (ITFS), and the algorithms employing functions that encourage orthogonality (FSFP-FSCA and UFS). They are also generally competitive with these other methods with respect to their native metrics, i.e. mutual information (MI) and frame potential (FP). Overall, L-FSCA/FSCA is the best performing algorithm across all case studies with regard to achieving the greatest data compression, as reflected in the AUC metric, followed closely by PFS. UFS and FSFP-FSCA are consistently the worst performing methods.

The development of L-FSCA was motivated by an assumption that while variance explained is not a submodular function, it is sufficiently close to being submodular in practice to warrant exploitation of an efficient *lazy* greedy implementation that is valid for such functions. The experimental evidence confirms the validity of this assumption with L-FSCA yielding almost identical results to FSCA for all 8 case studies investigated, and is therefore the algorithm of choice for unsupervised variable selection.

In terms of computational complexity, the most efficient algorithms among those considered are PFS (with principal components computed via NIPALS) and L-FSCA. As the complexity of the former and the latter are  $O(Nkmv)$  and  $O(kmv)$ , respectively, the fastest method is defined by the magnitude of the parameter  $N$ , which depends on the implementation of NIPALS.

The paper also reviewed several theoretical results from the field of combinatorial optimisation that provide performance guarantees for greedy search

algorithms with respect to the optimum solution for specific forms of selection function, starting with the classical  $\mathcal{B}_N > 63\%$  result by Nemhauser et al. [34] for submodular set functions, and then considering several results that apply to set functions that are close to being submodular, as expressed by characteristic properties such as curvature and submodularity ratio. Among these results the performance bound by Bian et al. [40] is shown to be the tightest bound for both submodular and non-submodular functions. While these bounds are generally conservative, and intractable to compute in practice, they help to validate the strong empirical performance of FSCA and L-FSCA.

### Acknowledgements

The first author gratefully acknowledges the financial support provided by Irish Manufacturing Research (IMR) for this research.

### References

- [1] K. A. Janes, M. B. Yaffe, Data-driven modelling of signal-transduction networks, *Nature reviews Molecular cell biology* 7 (11) (2006) 820–828.
- [2] S. Leonelli, Introduction: Making sense of data-driven research in the biological and biomedical sciences, *Studies in History and Philosophy of Biological and Biomedical Sciences* (2012).
- [3] G. Susto, A. Schirru, S. Pampuri, A. Beghi, A predictive maintenance system based on regularization methods for ion-implantation, in: 23rd IEEE/SEMI Advanced Semiconductor Manufacturing Conference, 2012, pp. 175–180.
- [4] J. Gonzaga, L. A. C. Meleiro, C. Kiang, R. Maciel Filho, ANN-based soft-sensor for real-time process monitoring and control of an industrial polymerization process, *Computers & Chemical Engineering* 33 (1) (2009) 43–49.

- [5] E. Delage, Y. Ye, Distributionally robust optimization under moment uncertainty with application to data-driven problems, *Operations research* 58 (3) (2010) 595–612.
- [6] S. Goonatilake, P. C. Treleaven, *Intelligent systems for finance and business*, John Wiley & Sons, Inc., 1995.
- [7] I. T. Jolliffe, *Principal component analysis and factor analysis*, in: *Principal component analysis*, Springer, 1986, pp. 115–128.
- [8] L. Van Der Maaten, E. Postma, J. Van den Herik, *Dimensionality reduction: a comparative review*, Technical Report TiCC-TR 2009-005, Tilburg University (2009).
- [9] A. Krause, A. Singh, C. Guestrin, Near-optimal sensor placements in gaussian processes: Theory, efficient algorithms and empirical studies, *Journal of Machine Learning Research* 9 (Feb) (2008) 235–284.
- [10] S. Mcloone, A. Johnston, G. A. Susto, A methodology for efficient dynamic spatial sampling and reconstruction of wafer profiles, *IEEE Transactions on Automation Science and Engineering* 15 (4) (2018) 1692–1703.
- [11] B. Flynn, S. McLoone, Max separation clustering for feature extraction from optical emission spectroscopy data, *IEEE Trans. Semicond. Manuf.* 24 (4) (2011) 480–488.
- [12] I. T. Jolliffe, N. T. Trendafilov, M. Uddin, A modified principal component technique based on the LASSO, *Journal of Computational and Graphical Statistics* 12 (3) (2003) 531–547.
- [13] A. d’Aspremont, L. E. Ghaoui, M. I. Jordan, G. R. Lanckriet, A direct formulation for sparse PCA using semidefinite programming, in: *Advances in neural information processing systems*, 2005, pp. 41–48.
- [14] H. Zou, T. Hastie, R. Tibshirani, Sparse principal component analysis, *Journal of computational and graphical statistics* 15 (2) (2006) 265–286.

- [15] D. M. Witten, R. Tibshirani, T. Hastie, A penalized matrix decomposition, with applications to sparse principal components and canonical correlation analysis, *Biostatistics* 10 (3) (2009) 515–534.
- [16] S. Joshi, S. Boyd, Sensor selection via convex optimization, *IEEE Transactions on Signal Processing* 57 (2) (2008) 451–462.
- [17] S. Liu, S. P. Chepuri, M. Fardad, E. Maşazade, G. Leus, P. K. Varshney, Sensor selection for estimation with correlated measurement noise, *IEEE Transactions on Signal Processing* 64 (13) (2016) 3509–3522.
- [18] S. P. Chepuri, G. Leus, Sparsity-promoting sensor selection for non-linear measurement models, *IEEE Transactions on Signal Processing* 63 (3) (2015) 684–698.
- [19] M. Masaeli, Y. Yan, Y. Cui, G. Fung, J. G. Dy, Convex principal feature selection, in: *Proceedings of the 2010 SIAM International Conference on Data Mining*, SIAM, 2010, pp. 619–628.
- [20] C. Waleesuksan, S. Wongsas, A fast variable selection for nonnegative garrote-based artificial neural network, in: *Electrical Engineering/Electronics, Computer, Telecommunications and Information Technology (ECTI-CON), 2016 13th International Conference on*, IEEE, 2016, pp. 1–6.
- [21] K. Sun, S.-H. Huang, D. S.-H. Wong, S.-S. Jang, Design and application of a variable selection method for multilayer perceptron neural network with LASSO, *IEEE transactions on neural networks and learning systems* 28 (6) (2017) 1386–1396.
- [22] K. Han, Y. Wang, C. Zhang, C. Li, C. Xu, Autoencoder inspired unsupervised feature selection, in: *2018 IEEE International Conference on Acoustics, Speech and Signal Processing (ICASSP)*, IEEE, 2018, pp. 2941–2945.
- [23] Y. Cui, J. G. Dy, Orthogonal principal feature selection (2008).

- [24] L. Puggini, S. McLoone, Forward selection component analysis: Algorithms and applications, *IEEE Transactions on Pattern Analysis and Machine Intelligence* 39 (12) (2017) 2395–2408.
- [25] S. Rao, S. P. Chepuri, G. Leus, Greedy sensor selection for non-linear models, in: *Computational Advances in Multi-Sensor Adaptive Processing (CAMSAP)*, 2015 IEEE 6th International Workshop on, IEEE, 2015, pp. 241–244.
- [26] A. Hashemi, M. Ghasemi, H. Vikalo, U. Topcu, Randomized greedy sensor selection: Leveraging weak submodularity, *IEEE Transactions on Automatic Control* (2020) 1–1.
- [27] M. Minoux, Accelerated greedy algorithms for maximizing submodular set functions, in: *Optimization techniques*, Springer, 1978, pp. 234–243.
- [28] P. K. Prakash, B. Honari, A. Johnston, S. F. McLoone, Optimal wafer site selection using forward selection component analysis, *ASMC (Advanced Semiconductor Manufacturing Conference) Proceedings* (2012) 91–96doi : 10.1109/ASMC.2012.6212875.
- [29] H.-L. Wei, S. A. Billings, Feature subset selection and ranking for data dimensionality reduction, *IEEE Transactions on Pattern Analysis and Machine Intelligence* 29 (1) (2007).
- [30] D. C. Whitley, M. G. Ford, D. J. Livingstone, Unsupervised forward selection: a method for eliminating redundant variables, *Journal of Chemical Information and Computer Sciences* 40 (5) (2000) 1160–1168.
- [31] J. Ranieri, A. Chebira, M. Vetterli, Near-optimal sensor placement for linear inverse problems, *IEEE Trans. Signal Process.* 62 (5) (2014) 1135–1146.
- [32] A. Das, D. Kempe, Algorithms for subset selection in linear regression, in: *Proceedings of the fortieth annual ACM symposium on Theory of computing*, ACM, 2008, pp. 45–54.



- [33] F. Zocco, S. McLoone, Mean squared error vs. frame potential for unsupervised variable selection, in: *Intelligent Computing, Networked Control, and Their Engineering Applications*, Springer, pp. 353–362, 2017.
- [34] G. L. Nemhauser, L. A. Wolsey, M. L. Fisher, An analysis of approximations for maximizing submodular set functions—i, *Mathematical Programming* 14 (1) (1978) 265–294.
- [35] M. Conforti, G. Cornuéjols, Submodular set functions, matroids and the greedy algorithm: tight worst-case bounds and some generalizations of the rado-edmonds theorem, *Discrete applied mathematics* 7 (3) (1984) 251–274.
- [36] R. K. Iyer, S. Jegelka, J. A. Bilmes, Curvature and optimal algorithms for learning and minimizing submodular functions, in: *Advances in Neural Information Processing Systems*, 2013, pp. 2742–2750.
- [37] M. Sviridenko, J. Vondrák, J. Ward, Optimal approximation for submodular and supermodular optimization with bounded curvature, *Mathematics of Operations Research* 42 (4) (2017) 1197–1218.
- [38] A. Das, D. Kempe, Submodular meets spectral: Greedy algorithms for subset selection, sparse approximation and dictionary selection, *International Conference on Machine Learning Research* (2011).
- [39] A. Das, D. Kempe, Approximate submodularity and its applications: Subset selection, sparse approximation and dictionary selection, *The Journal of Machine Learning Research* 19 (1) (2018) 74–107.
- [40] A. A. Bian, J. M. Buhmann, A. Krause, S. Tschieschek, Guarantees for greedy maximization of non-submodular functions with applications, in: *International conference on machine learning*, PMLR, 2017, pp. 498–507.
- [41] Z. Wang, B. Moran, X. Wang, Q. Pan, Approximation for maximizing monotone non-decreasing set functions with a greedy method, *Journal of Combinatorial Optimization* 31 (1) (2016) 29–43.

- [42] A. Hashemi, M. Ghasemi, H. Vikalo, U. Topcu, Submodular observation selection and information gathering for quadratic models, in: International Conference on Machine Learning, PMLR, 2019, pp. 2653–2662.
- [43] E. Ragnoli, S. McLoone, S. Lynn, J. Ringwood, N. Macgearailt, Identifying key process characteristics and predicting etch rate from high-dimension datasets, in: Advanced Semiconductor Manufacturing Conference, 2009. ASMC'09. IEEE/SEMI, IEEE, 2009, pp. 106–111.
- [44] G. A. Susto, M. Maggipinto, F. Zocco, S. McLoone, Induced start dynamic sampling for wafer metrology optimization, *IEEE Trans. Autom. Sci. Eng.* 17 (1) (2019) 418–432.
- [45] R. B. Bendel, A. A. Afifi, Comparison of stopping rules in forward “step-wise” regression, *Journal of the American Statistical association* 72 (357) (1977) 46–53.
- [46] K. Kersting, C. Plagemann, P. Pfaff, W. Burgard, Most likely heteroscedastic gaussian process regression, in: Proceedings of the 24th international conference on Machine learning, ACM, 2007, pp. 393–400.
- [47] H. Wold, Nonlinear iterative partial least squares (NIPALS) modelling: Some current developments, in: *Multivariate Analysis–III*, Elsevier, 1973, pp. 383–407.
- [48] J. Jeffers, Two case studies in the application of principal component analysis, *Applied Statistics* (1967) 225–236.
- [49] H. A. Guvenir, B. Acar, G. Demiroz, A. Cekin, A supervised machine learning algorithm for arrhythmia analysis, in: *Computers in Cardiology*, 1997, pp. 433–436.
- [50] S. C. Tan, J. P. San Lau, Time series clustering: A superior alternative for market basket analysis, in: Proceedings of the First International Conference on Advanced Data and Information Engineering (DaEng-2013), Springer, Singapore, 2014, pp. 241–248.

- [51] S. C. Tan, P. San Lau, X. Yu, Finding similar time series in sales transaction data, in: International Conference on Industrial, Engineering and Other Applications of Applied Intelligent Systems, Springer, Cham, 2015, pp. 645–654.
- [52] A. Vergara, S. Vembu, T. Ayhan, M. A. Ryan, M. L. Homer, R. Huerta, Chemical gas sensor drift compensation using classifier ensembles, Sensors and Actuators B: Chemical 166 (2012) 320–329.
- [53] I. Rodriguez-Lujan, J. Fonollosa, A. Vergara, M. Homer, R. Huerta, On the calibration of sensor arrays for pattern recognition using the minimal number of experiments, Chemometrics and Intelligent Laboratory Systems 130 (2014) 123–134.
- [54] F. Zhou, Q. Claire, R. D. King, Predicting the geographical origin of music, in: 2014 IEEE international conference on data mining (ICDM), IEEE, 2014, pp. 1115–1120.